Internet Appendix

"High Volatility is the Key: A Joint Treatment of Asset Pricing Puzzles"

Errikos Melissinos

The main article is available at https://errikos-melissinos.com/pdfs/High_Volatility_is_the_Key_A_Joint_Treatment_of_Asset_Pricing_Puzzles.pdf.

This Internet Appendix consists of three parts. Section IA.A provides a review of the literature on the bond premium puzzle. Section IA.B presents a self-contained mathematical framework for the model variations analyzed in this appendix. Section IA.C documents yield and term-premium results for all 37 model variations, together with a model index table. This appendix is adapted from an earlier working-paper version of this article and is included here because the main text makes reference to it. Its model variations and calibrations predate the baseline calibration of the main text and share no parameter values with it. The appendix documents qualitative conclusions, in particular that standard models do not generate positive real term premia across a wide range of specifications, and its numbers should not be compared with those of the main text.

IA.A Literature on the Bond Premium Puzzle

This section reviews available explanations of the bond premium puzzle.[1] One of the first papers to address this was Backus, Gregory and Zin 1989. Utilizing a consumption-based asset-pricing model of an endowment economy, they discovered the model's inability to yield significant positive term premia. Subsequent studies

[1]Rudebusch and Swanson 2008 provides a good summary of this extensive literature.

by Donaldson, Johnsen and Mehra 1990 and Den Haan 1995 further indicated that standard real business cycle models also could not resolve the puzzle. Rudebusch and Swanson 2008 incorporated an external habit into DSGE models but found that the bond premium puzzle remains. Duffee 2013 showed that basic properties of nominal yields cannot be explained macroeconomically. Also, Duffee 2002 shed light on the challenges of fitting both interest rate and term premium dynamics within affine models.

Next, a series of papers provided explanations focused on nominal term premia. Notably, Piazzesi and Schneider 2006 showed that parameter uncertainty in a model where inflation brings bad news about future consumption growth can produce positive nominal term premia.[2] Gabaix 2012 and Tsai 2015, following Rietz 1988 and Barro 2006, showed that positive nominal term premia can be explained if inflation is on average high during consumption disasters. Bansal and Shaliastovich 2013, following Bansal and Yaron 2004, demonstrated that the risk premium of a nominal bond can be positive when inflation is correlated with consumption trend. Rudebusch and Swanson 2012 used a similar model within a DSGE framework that generates positive nominal term premia, but real term premia are negative. Gomez-Cram and Yaron 2021 also used a long-run risk model focused on nominal term premia.

Alternatively, some articles consider real term premia. Katagiri 2022 explored a model with monetary policy in which consumption changes can be negatively correlated with consumption trends and risk aversion is very high. Ellison and Tischbirek 2021 used a beauty-contest mechanism as in Angeletos, Collard and Dellas 2018, in which agents anticipate others' expectations, generating positive term premia.

Using an approach similar to the main article, some papers deviate from

[2] Collin-Dufresne, Johannes and Lochstoer 2016 introduced a model with Bayesian learning of parameters that generates negative term premia.

the representative agent model. Vayanos and Vila 2021 suggested that term premia are generated by arbitrageurs interacting with preferred-habitat investors. Kekre, Lenel and Mainardi 2024 built on Vayanos and Vila 2021 and showed that arbitrageur portfolio characteristics have important implications for the sign of term premia. Jappelli, Pelizzon and Subrahmanyam 2024 extended this by integrating the repo market. Schneider 2022 showed that positive term premia can arise in models with heterogeneous agents exhibiting different risk attitudes and intertemporal substitution preferences.[3] Finally, returning to representative-agent models, Wachter 2006 showed that term premia can be positive and time-varying in a model with external habit following Campbell and Cochrane 1999. Kliem and Meyer-Gohde 2022 and Hsu, Li and Palomino 2021 used the same mechanism within DSGE models. Campbell, Pflueger and Viceira 2020 also used a habit model to explain the time-variability of term premia. More generally, Lettau and Wachter 2011 and Bekaert, Engstrom and Grenadier 2010 showed that positive and time-varying term premia can be obtained within the class of models with time-varying effective risk aversion. To the authors' knowledge, time-varying risk aversion is the only mechanism in the literature that achieves positive and time-varying term premia within a rational representative agent model.

IA.B Mathematical Framework

A consumption-based framework in continuous time accommodates a range of model variations. The framework is built upon three components: (1) an exogenous consumption process, (2) a utility specification, and (3) a process for the state variable. The state variable determines the state of the economy, and is connected to either the consumption drift (CD), the consumption volatility (CV), or the external habit. Utility is either time-separable (TSU) or recursive (RU), the latter

[3] Schneider 2022 also uses effective time-varying risk aversion.

following Duffie and Epstein 1992.

IA.B.1 Consumption process

Consumption (C_t) follows the stochastic process:

$$\mathrm{d}\log(C_t) = \mathrm{d}c_t = \mu_{ct}\,\mathrm{d}t + \sigma_{ct}\,\mathrm{d}W_{ct} \tag{IA.1}$$

where μ_{ct} denotes the consumption drift at time t and σ_{ct} is the consumption volatility, multiplying the standard Wiener process $\mathrm{d}W_{ct}$.

IA.B.2 Utility

Lifetime utility takes the following form depending on the specification:

$$\underbrace{U_0 = \mathrm{E}_0 \int_0^\infty e^{-\rho t} u(C_t, S_t)\,\mathrm{d}t,}_{\text{TSU}} \qquad \underbrace{V_0 = \mathrm{E}_0 \int_0^\infty F(C_t, V_t)\,\mathrm{d}t}_{\text{RU}} \tag{IA.2}$$

where ρ is the time preference parameter. In the TSU case, flow utility u depends on consumption and potentially on the surplus consumption ratio S_t (relevant only in the habit model; set to 1 otherwise). In the RU case, F is the Duffie–Epstein aggregator depending on consumption and the current value function V_t. The functional forms are:

$$\begin{aligned} u(C_t, S_t) &= \frac{(C_t S_t)^{1-\gamma} - 1}{1-\gamma} \qquad \text{(TSU)} \\ F(C_t, V_t) &= \frac{\rho\,(1-\gamma)\,V_t}{1-1/\psi}\left(\left(\frac{C_t}{((1-\gamma)\,V_t)^{-1/(1-\gamma)}}\right)^{1-1/\psi} - 1\right) \qquad \text{(RU)} \end{aligned} \tag{IA.3}$$

Here γ is risk aversion (equal to the inverse of the IES in TSU), and ψ is the IES in the RU case.

IA.B.3 State variable

The state variable x_t follows a mean-reverting process:

$$\mathrm{d}x_t = -\log(\phi)(\mu_{x0} - x_t)\,\mathrm{d}t + \sigma_{xt}\,\mathrm{d}W_{xt} \tag{IA.4}$$

where μ_{x0} is the steady state and $\phi \in (0,1)$ governs mean reversion. The Wiener process $\mathrm{d}W_{xt}$ has correlation ρ_{cx} with $\mathrm{d}W_{ct}$. Table IA.1 shows how each model variation maps the state variable into the consumption and state processes.

Table IA.1: **State variable dependence for each model variation**

Model variation			
TSU-CD:	$\mu_{ct} = \mu_{c0} + x_t$	$\sigma_{xt} = \sigma_{x0}$	$\mu_{x0} = 0$
TSU-CV:	$\sigma_{ct} = \sigma_{c1} x_t$	$\sigma_{xt} = \sigma_{x1}\sqrt{x_t}$	$\mu_{x0} = 1$
TSU-Habit:*	$S_t = \bar{S}e^{x_t}$	$\sigma_{xt} = \sigma_{ct}\lambda(x_t)$	$\mu_{x0} = 0$
RU-CD:	$\mu_{ct} = \mu_{c0} + x_t$	$\sigma_{xt} = \sigma_{x0}$	$\mu_{x0} = 0$
RU-CV:	$\sigma_{ct} = \sigma_{c1}\sqrt{x_t}$	$\sigma_{xt} = \sigma_{x1}\sqrt{x_t}$	$\mu_{x0} = 1$
TSU-HCV:	$\sigma_{ct} = \sigma_{c1} x_t$	$\sigma_{xt} = \sigma_{x1}\sqrt{x_t}$	$\mu_{x0} = 1$
Arb-IN:	$\mu_{ct} = \mu_{c1} x_t^{1/4}$, $\sigma_{ct} = \sigma_{c1}\sqrt{x_t}$	$\sigma_{xt} = \sigma_{x1}\sqrt{x_t}$	$\mu_{x0} = 1$
Arb-DP:	$\mu_{ct} = \mu_{c1} x_t^{3/2}$, $\sigma_{ct} = \sigma_{c1} x_t^{2/3}$	$\sigma_{xt} = \sigma_{x1}\sqrt{x_t}$	$\mu_{x0} = 1$

* Following Campbell and Cochrane 1999 and Wachter 2006:

$$\sigma_{xt} = \sigma_{ct}\lambda(x_t) = \begin{cases} \sigma_{ct}\left(\dfrac{\sqrt{1-2x_t}}{\bar{S}} - 1\right) & \text{if } x_t < \dfrac{1-\bar{S}^2}{2} \\ 0 & \text{if } x_t \geq \dfrac{1-\bar{S}^2}{2} \end{cases}, \quad \bar{S} = \sqrt{\frac{\gamma}{-\log(\phi) - b/\gamma}}$$

In variations where consumption volatility σ_{ct} is proportional to the state variable, the steady state is set at $x_t = 1$ (with $x_t > 0$ almost surely), ensuring positivity of σ_{ct}.

IA.B.4 Stochastic discount factor

Time-separable utility. The SDF is the derivative of flow utility with respect to consumption:

$$\Lambda_t = e^{-\rho t}(C_t S_t)^{-\gamma} \tag{IA.5}$$

Applying Itô's Lemma yields the SDE:

$$\begin{aligned}\frac{\mathrm{d}\Lambda_t}{\Lambda_t} =& \Big(-\rho - \gamma\mu_{ct} + \tfrac{\gamma^2}{2}\sigma_{ct}^2\Big)\mathrm{d}t - \gamma\sigma_{ct}\,\mathrm{d}W_{ct} \\ & \underbrace{+\big(-\gamma\log(\phi)x_t + 2\rho_{cx}\sigma_{ct}\sigma_{xt} + \sigma_{xt}^2\big)\mathrm{d}t - \gamma\sigma_{xt}\,\mathrm{d}W_{xt}}_{\text{habit model only}} \end{aligned} \tag{IA.6}$$

Recursive utility. Following Tsai and Wachter 2018, the value function takes the form:

$$V_t = \frac{C_t^{1-\gamma}e^{(1-\gamma)K(x_t)}}{1-\gamma} \tag{IA.7}$$

where $K(x_t)$ captures the full dependence of the value function on the state variable (see Section IA.B.8 for the perturbation method to solve for K). The SDF is derived from the aggregator F as:

$$\begin{aligned}\frac{\mathrm{d}\Lambda_t}{\Lambda_t} =& \Bigg(\frac{\rho\left((1-\gamma\psi)e^{\frac{(1-\psi)K[x_t]}{\psi}} + \gamma\psi - \psi\right)}{1-\psi} - \gamma\mu_{ct} + \frac{\gamma^2\sigma_{ct}^2}{2} \\ & + \frac{\gamma(\gamma\psi-1)\rho_{cx}\sigma_{xt}\sigma_{ct}K'(x_t)}{\psi} \\ & + \frac{(\gamma\psi-1)\left(2\psi(\mu_{x0}-x_t)\log(\phi)K'(x_t) + \sigma_{xt}^2\left((\gamma\psi-1)K'(x_t)^2 - \psi K''(x_t)\right)\right)}{2\psi^2}\Bigg)\mathrm{d}t \\ & - \frac{(\gamma\psi-1)\sigma_{xt}K'(x_t)}{\psi}\,\mathrm{d}W_{xt} - \gamma\sigma_{ct}\,\mathrm{d}W_{ct} \end{aligned} \tag{IA.8}$$

When $\gamma = 1/\psi$ this reduces to the TSU formula.

IA.B.5 Short-term interest rate

The short rate is $r(x_t) = -\mathrm{E}_t[\mathrm{d}\Lambda_t/\Lambda_t]/\mathrm{d}t$. For TSU:

$$r(x_t) = \rho + \gamma\mu_{ct} - \tfrac{\gamma^2}{2}\sigma_{ct}^2 \underbrace{-\gamma\log(\phi)x_t + 2\rho_{cx}\sigma_{ct}\sigma_{xt} + \sigma_{xt}^2}_{\text{habit model only}} \tag{IA.9}$$

For RU:

$$
\begin{aligned}
r(x_t) = {} & \frac{\rho\left((1-\gamma\psi)e^{\frac{(1-\psi)K[x_t]}{\psi}} + \gamma\psi - \psi\right)}{1-\psi} + \gamma\mu_{ct} - \frac{\gamma^2\sigma_{ct}^2}{2} \\
& - \frac{\gamma(\gamma\psi-1)\rho_{cx}\sigma_{xt}\sigma_{ct}K'(x_t)}{\psi} \\
& - \frac{(\gamma\psi-1)\left(2\psi(\mu_{x0}-x_t)\log(\phi)K'(x_t) + \sigma_{xt}^2\left((\gamma\psi-1)K'(x_t)^2 - \psi K''(x_t)\right)\right)}{2\psi^2}
\end{aligned}
\tag{IA.10}
$$

IA.B.6 Bond pricing

The price $Q(x_t, m)$ of a zero-coupon bond with remaining maturity m satisfies the PDE:

$$
-Q_m - r(x_t)Q + \big(-\log(\phi)(\mu_{x0} - x_t) + A(x_t)\big)Q_x + \frac{\sigma_{xt}^2}{2}Q_{xx} = 0 \tag{IA.11}
$$

where subscripts denote partial derivatives and $A(x_t)\,\mathrm{d}t \equiv (\mathrm{d}\Lambda_t/\Lambda_t)(\mathrm{d}Q)$ is the covariance between the SDF and the bond price (i.e., the source of the term premium). The terminal condition is $Q(x_t, 0) = 1$.

The solution is given by the Feynman–Kac formula:

$$
Q(m, x_t) = \mathrm{E}_t\left[\exp\left\{-\int_0^m r(\tilde{x}_{t+s})\,\mathrm{d}s\right\}\right] \tag{IA.12}
$$

where $\tilde{x}$ follows the risk-adjusted process:

$$
\mathrm{d}\tilde{x}_t = \Big(-\log(\phi)(\mu_{x0} - \tilde{x}_t) + A(\tilde{x}_t)\Big)\mathrm{d}t + \sigma_{xt}(\tilde{x}_t)\,\mathrm{d}W_{xt} \tag{IA.13}
$$

This expectation is computed via Monte Carlo simulation.

IA.B.7 Risk-neutral yield and term premium

Setting $A \equiv 0$ gives the risk-neutral bond price:

$$H(m, x_t) = \mathrm{E}_t\left[\exp\left\{-\int_0^m r(x_{t+s})\,\mathrm{d}s\right\}\right] \tag{IA.14}$$

The term premium of maturity m is:

$$TP(x_t, m) = \frac{-\log Q(x_t, m) - (-\log H(x_t, m))}{m} \tag{IA.15}$$

IA.B.8 Perturbation approximation for K (recursive utility)

In the RU case, $K(x_t)$ is the solution of the following ordinary differential equation (ODE), obtained by substituting the value function into the Hamilton–Jacobi–Bellman equation with $\psi = 1/(1-\epsilon)$:

$$\begin{aligned} -\tfrac{1}{2}\gamma\sigma_{ct}^2 + \tfrac{1}{2}\sigma_{xt}^2\big(K''(x_t) - (\gamma-1)K'(x_t)^2\big) - \log(\phi)(\mu_{x0} - x_t)K'(x_t) \\ + \frac{\rho(e^{-\epsilon K(x_t)} - 1)}{\epsilon} + \mu_{ct} = 0 \end{aligned} \tag{IA.16}$$

For $\psi = 1$ (i.e. $\epsilon = 0$) this ODE has an analytic solution $K_0(x_t)$. Expanding K in powers of ϵ:

$$K(x_t; \epsilon) = K_0(x_t) + \epsilon\, K_1(x_t) + \epsilon^2\, K_2(x_t) + \cdots \tag{IA.17}$$

and substituting into (IA.16), each K_n is a polynomial in x_t of degree $n+1$:

$$\begin{aligned}
K_0(x_t) &= a_{0,0} + a_{0,1}x_t \\
K_1(x_t) &= a_{1,0} + a_{1,1}x_t + a_{1,2}x_t^2 \\
K_2(x_t) &= a_{2,0} + a_{2,1}x_t + a_{2,2}x_t^2 + a_{2,3}x_t^3 \\
&\vdots
\end{aligned} \tag{IA.18}$$

The coefficients $a_{m,n}$ are determined by matching powers of $x_t^m \epsilon^n$ to zero, yielding a sequence of linear equations that can be solved successively. This provides a global approximation in the state variable for a wide range of IES values. The approach extends Tsai and Wachter 2018, who derived only the zeroth-order term K_0; higher-order terms enable accurate approximations well away from $\psi = 1$.[4]

IA.C Model Variations: Yields and Term Premia

This section presents yield and term premium results for all 37 model variations. Each figure has four panels, with the respective state variable on the x-axis. The top-left panel shows the instantaneous rate, the five-year yield, and the five-year risk-neutral yield. The top-right panel shows the decomposition of the five-to-ten-year forward rate into the full yield, the risk-neutral yield, and the term premium. The bottom-left panel shows the instantaneous, five-year, and ten-year yields. The bottom-right panel shows the term premia for three-, five-, and ten-year bonds. The solid vertical line marks the ergodic median; dashed vertical lines show the 10th-percentile minimum and 90th-percentile maximum over 12-year simulations, so that 90% of simulated paths lie within the boundaries.

[4] One limitation is that σ_{xt}^2 and σ_{ct}^2 must be at most linear in x_t, so unlike in the TSU case where $\sigma_{ct} \propto x_t$, the RU case requires $\sigma_{ct} \propto \sqrt{x_t}$, somewhat restricting the variability of consumption volatility.

IA.C.1 Model index

Abbreviations used: time-varying (TV), consumption drift (CD), consumption volatility (CV), time-separable utility (TSU), recursive utility (RU), intertemporal elasticity of substitution (IES).

Model Variation Description	**Abbreviation**	**Reference**
Time-separable utility (TSU)		
TV CD with TSU.	TSU-CD	Figure IA.1
TV CD with TSU and high risk aversion.	TSU-CD-HRA	Figure IA.2
TV CD with TSU and low persistence.	TSU-CD-LP	Figure IA.3
TV CD with TSU and high correlation ρ_{cx}.	TSU-CD-HCor	Figure IA.4
TV CD with TSU and high impatience.	TSU-CD-HImp	Figure IA.5
TV and high CD with TSU.	TSU-HCD	Figure IA.6
TV CD with TSU and high CV.	TSU-CD-HCV	Figure IA.7
TV CV with TSU.	TSU-CV	Figure IA.8
TV CV with TSU and high risk aversion.	TSU-CV-HRA	Figure IA.9
TV CV with TSU and high CD.	TSU-CV-HCD	Figure IA.10
TV and HCV with TSU and positive ρ_{cx}.	TSU-HCV	Figure IA.11
TV and HCV with TSU and negative ρ_{cx}.	TSU-HCV-NCor	Figure IA.12
Both TV CD and CV, rate decreasing in CV and ρ_{cx} positive.	TSU-Arb-DP	Figure IA.13
Both TV CD and CV, rate increasing in CV and ρ_{cx} negative.	TSU-Arb-IN	Figure IA.14
Both TV CD and CV, rate decreasing in CV and ρ_{cx} negative.	TSU-Arb-DN	Figure IA.15
Both TV CD and CV, rate increasing in CV and ρ_{cx} positive.	TSU-Arb-IP	Figure IA.16
TV external habit with TSU.	TSU-Habit	Figure IA.17
TV external habit with TSU and low b.	TSU-Habit-Low.b	Figure IA.18
TV external habit with TSU and $b < 0$.	TSU-Habit-Neg.b	Figure IA.19
TV external habit with TSU and constant state volatility.	TSU-Habit-CSV	Figure IA.20

Table IA.2: **Index of model variations (Part I: time-separable utility).**

Model Variation Description	Abbreviation	Reference
Recursive utility (RU)		
TV CD with RU.	RU-CD	Figure IA.21
TV CD with RU and high risk aversion.	RU-CD-HRA	Figure IA.22
TV CD with RU and high IES.	RU-CD-HIES	Figure IA.23
TV CD with RU and low IES.	RU-CD-LIES	Figure IA.24
TV CD with RU and high ρ_{cx}.	RU-CD-HCor	Figure IA.25
TV CD with RU and negative ρ_{cx}.	RU-CD-NCor	Figure IA.26
TV and high CD with RU.	RU-HCD	Figure IA.27
TV CD with RU and high CV.	RU-CD-HCV	Figure IA.28
TV and heteroskedastic CD with RU and ρ_{cx} positive.	RU-CD-Heterosk-PCor	Figure IA.29
TV and heteroskedastic CD with RU and ρ_{cx} negative.	RU-CD-Heterosk-NCor	Figure IA.30
TV CV with RU.	RU-CV	Figure IA.31
TV CV with RU and high risk aversion.	RU-CV-HRA	Figure IA.32
TV CV with RU and high persistence.	RU-CV-HP	Figure IA.33
TV CV with RU and high IES.	RU-CV-HIES	Figure IA.34
TV CV with RU and low IES.	RU-CV-LIES	Figure IA.35
TV and HCV with RU and ρ_{cx} positive.	RU-HCV-PCor	Figure IA.36
TV and HCV with RU and ρ_{cx} negative.	RU-HCV-NCor	Figure IA.37

Table IA.3: **Index of model variations (Part II: recursive utility).**

IA.C.2 TSU-CD (baseline calibration used in main article)

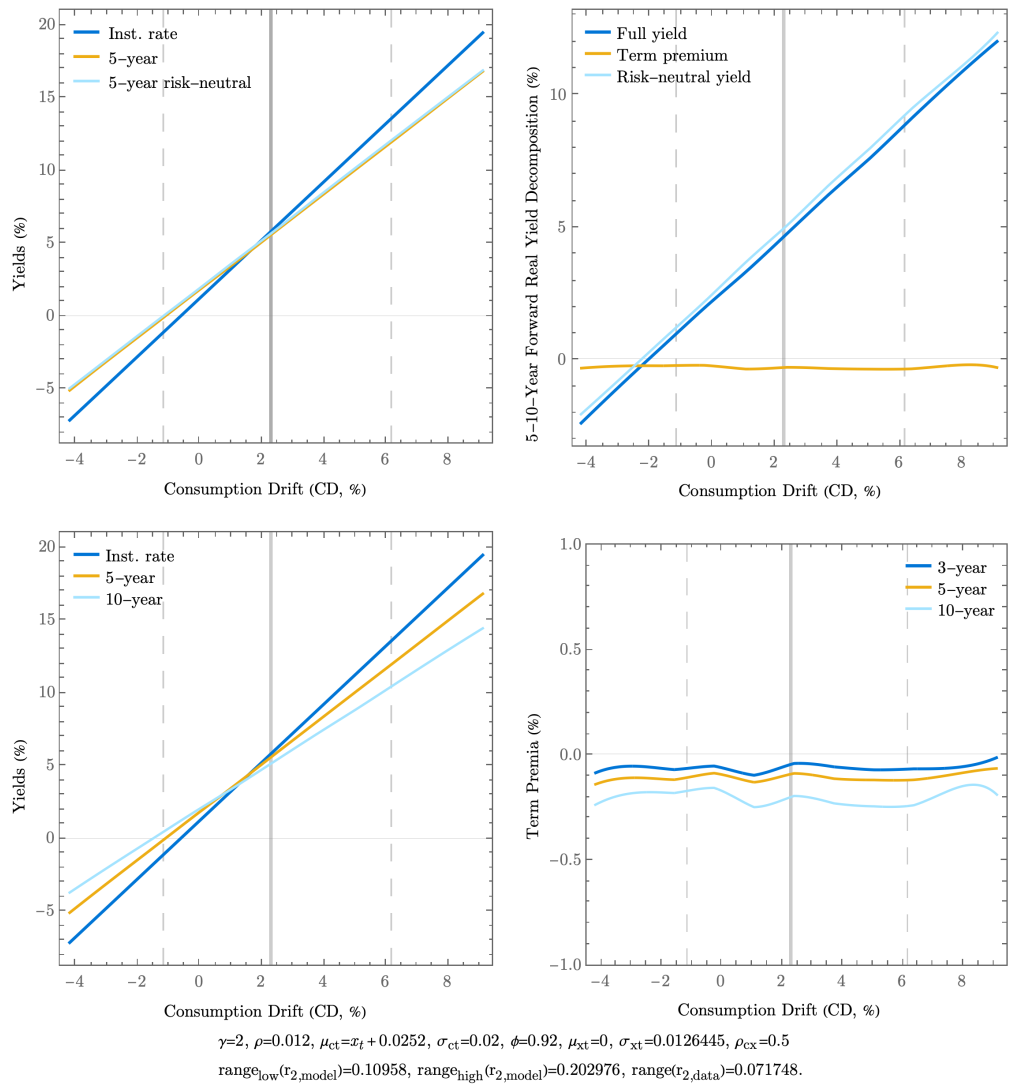

Figure IA.1: Time-varying CD with TSU. Top-left: instantaneous rate, 5-year yield, and 5-year risk-neutral yield as functions of consumption drift (or the respective state variable in other figures). Top-right: 5–10-year forward real yield decomposed into full yield, risk-neutral yield, and term premium. Bottom-left: instantaneous, 5-year, and 10-year yields. Bottom-right: term premia for 3-, 5-, and 10-year bonds. The solid vertical line marks the ergodic median; dashed vertical lines show the 10th-percentile minimum and 90th-percentile maximum over 12-year simulations.

IA.C.3 TSU-CD-HRA, $\gamma = 8$

Term premia are slightly larger but remain negative and constant with respect to the state variable.

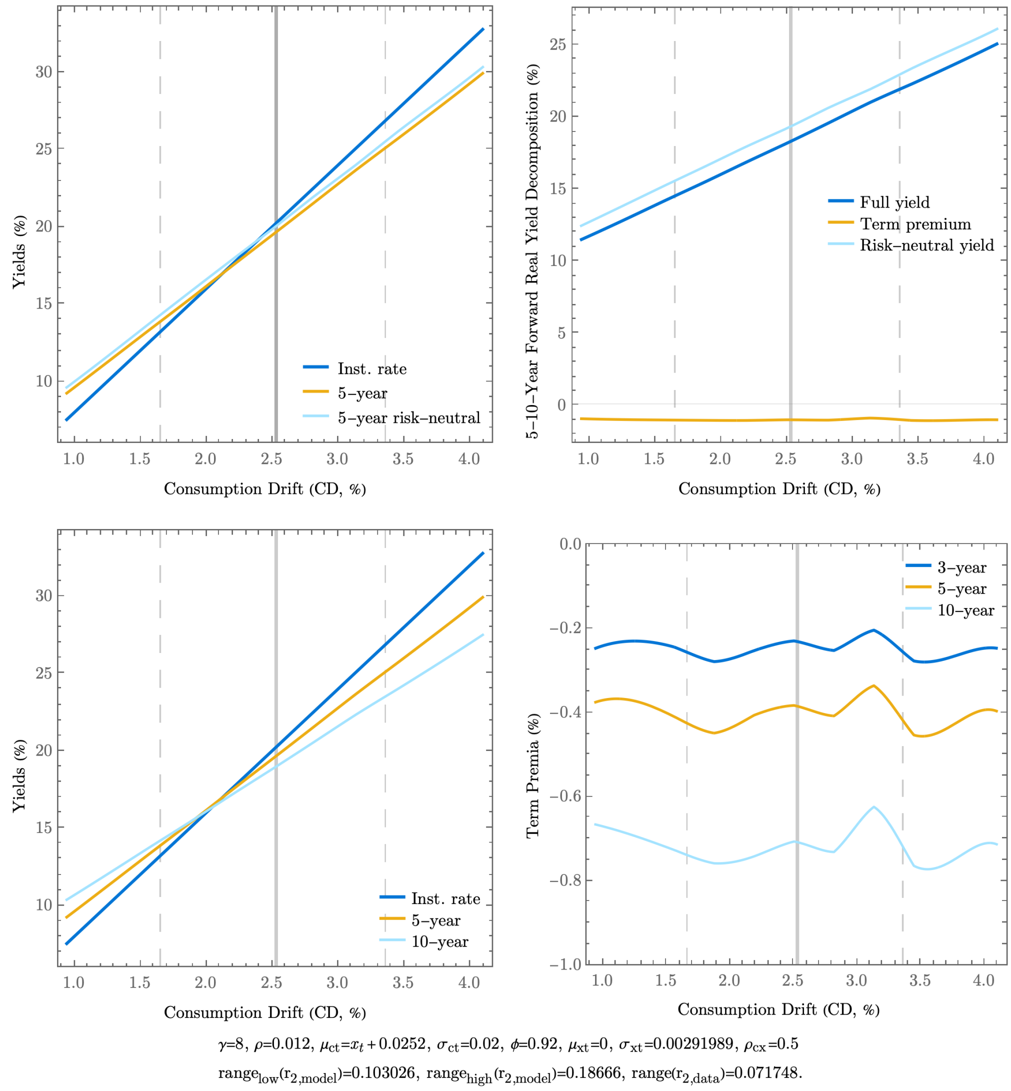

Figure IA.2: Time-varying CD with TSU and higher risk aversion. See Figure IA.1 for plot details.

IA.C.4 TSU-CD-LP, $\phi = 0.8$

Term premia are unchanged. There is larger separation between yields, consistent with the expectation mechanism.

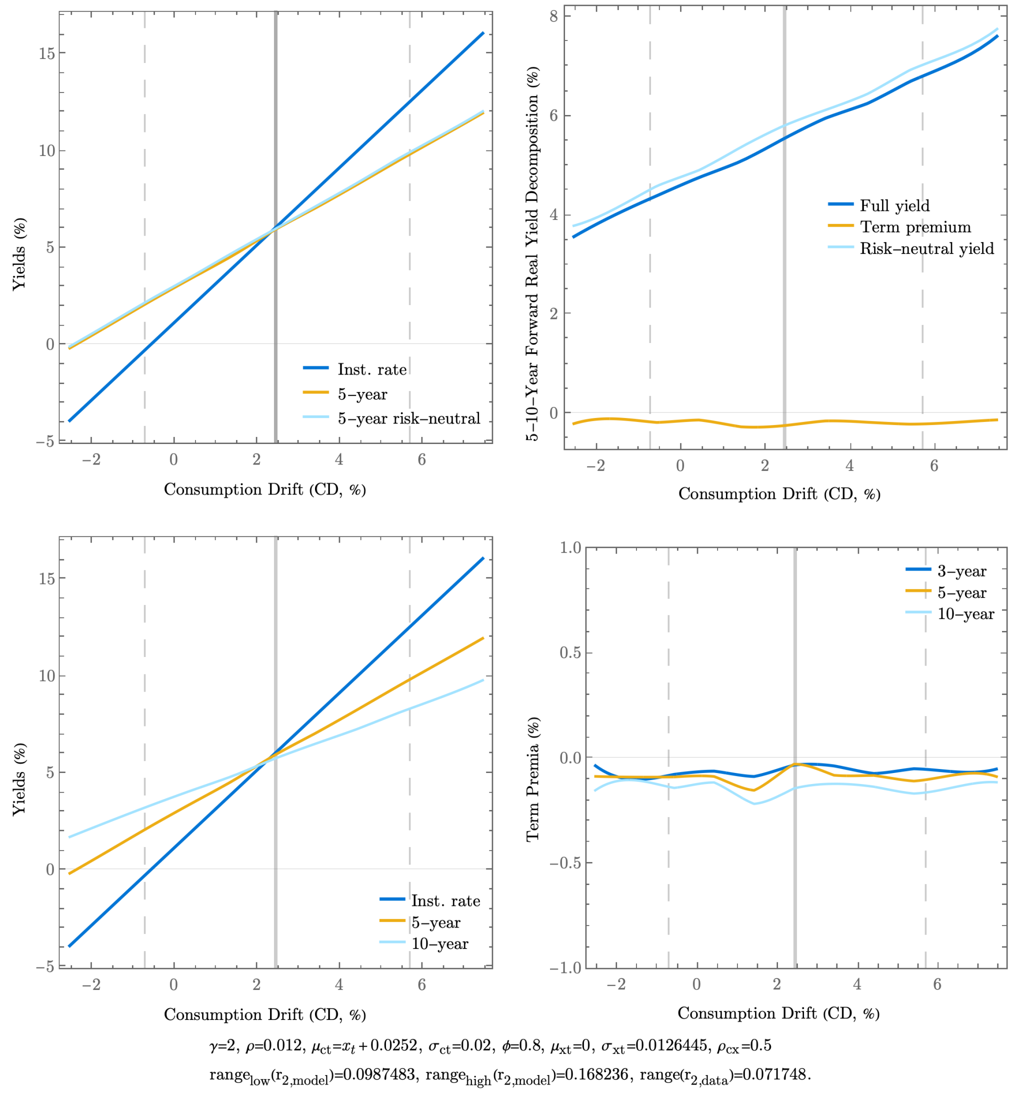

Figure IA.3: Time-varying CD with TSU and low persistence. See Figure IA.1 for plot details.

IA.C.5 TSU-CD-HCor, $\rho_{cx} = 1$

Term premia are larger in absolute value.

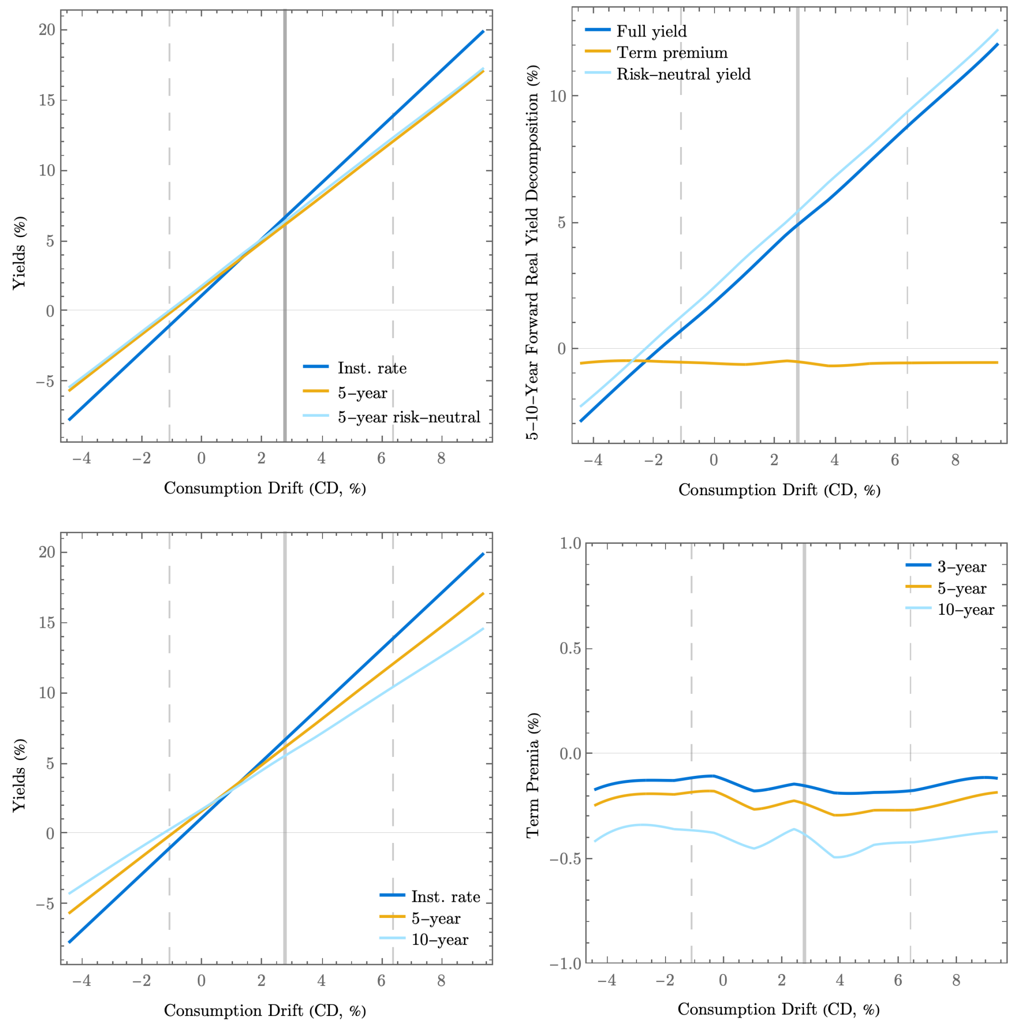

γ=2, ρ=0.012, $\mu_{ct}=x_t+0.0252$, σ_{ct}=0.02, ϕ=0.92, μ_{xt}=0, σ_{xt}=0.0126445, ρ_{cx}=1

$\text{range}_{\text{low}}(r_{2,\text{model}})$=0.111377, $\text{range}_{\text{high}}(r_{2,\text{model}})$=0.203865, $\text{range}(r_{2,\text{data}})$=0.071748.

Figure IA.4: Time-varying CD with TSU and high correlation ρ_{cx}. See Figure IA.1 for plot details.

IA.C.6 TSU-CD-HImp, $\rho = 0.05$

Yields shift higher without any change in term premia.

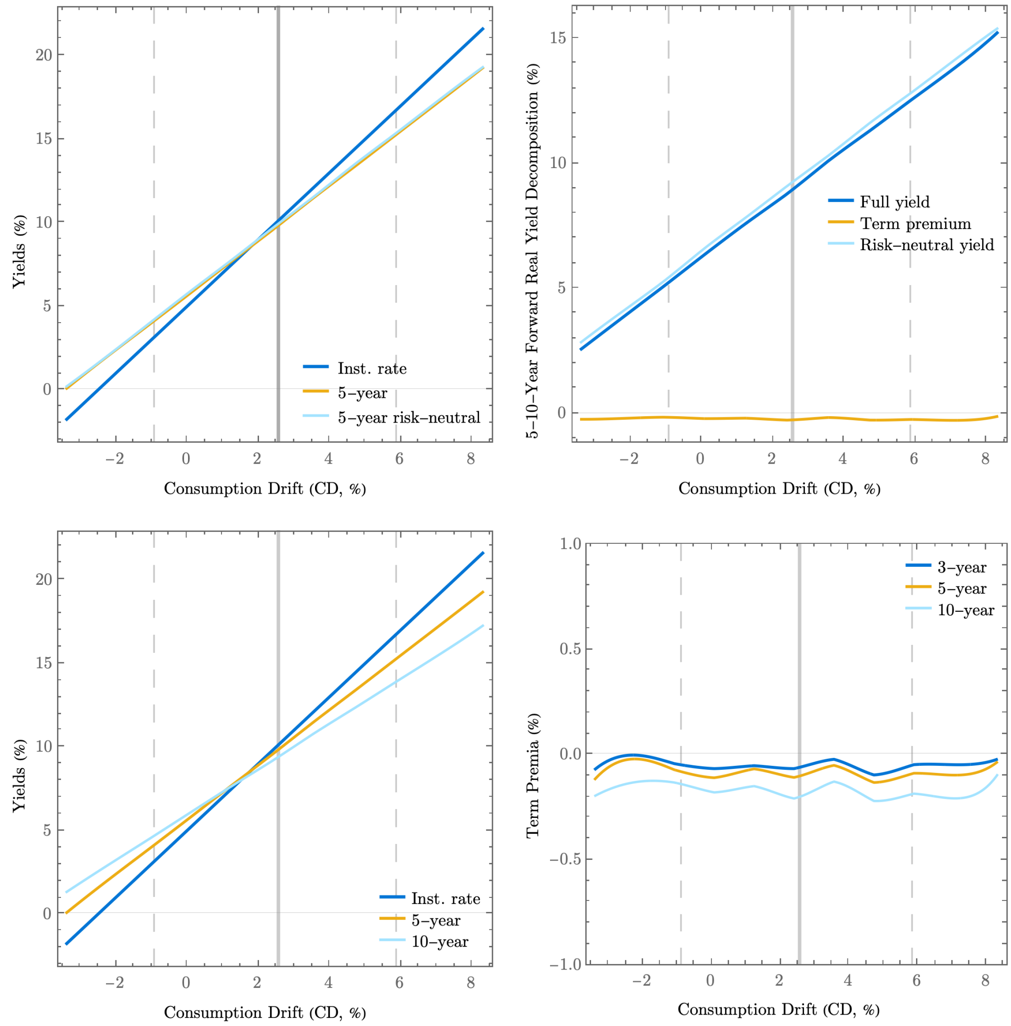

γ=2, ρ=0.05, μ_{ct}=x_t + 0.0252, σ_{ct}=0.02, ϕ=0.92, μ_{xt}=0, σ_{xt}=0.011495, ρ_{cx}=0.5

$\mathrm{range}_{\mathrm{low}}(\mathrm{r}_{2,\mathrm{model}})$=0.0973497, $\mathrm{range}_{\mathrm{high}}(\mathrm{r}_{2,\mathrm{model}})$=0.182416, $\mathrm{range}(\mathrm{r}_{2,\mathrm{data}})$=0.071748.

Figure IA.5: Time-varying CD with TSU and high impatience. See Figure IA.1 for plot details.

IA.C.7 TSU-HCD, $\mu_{c0} = 0.06$

Yields shift higher without any change in term premia.

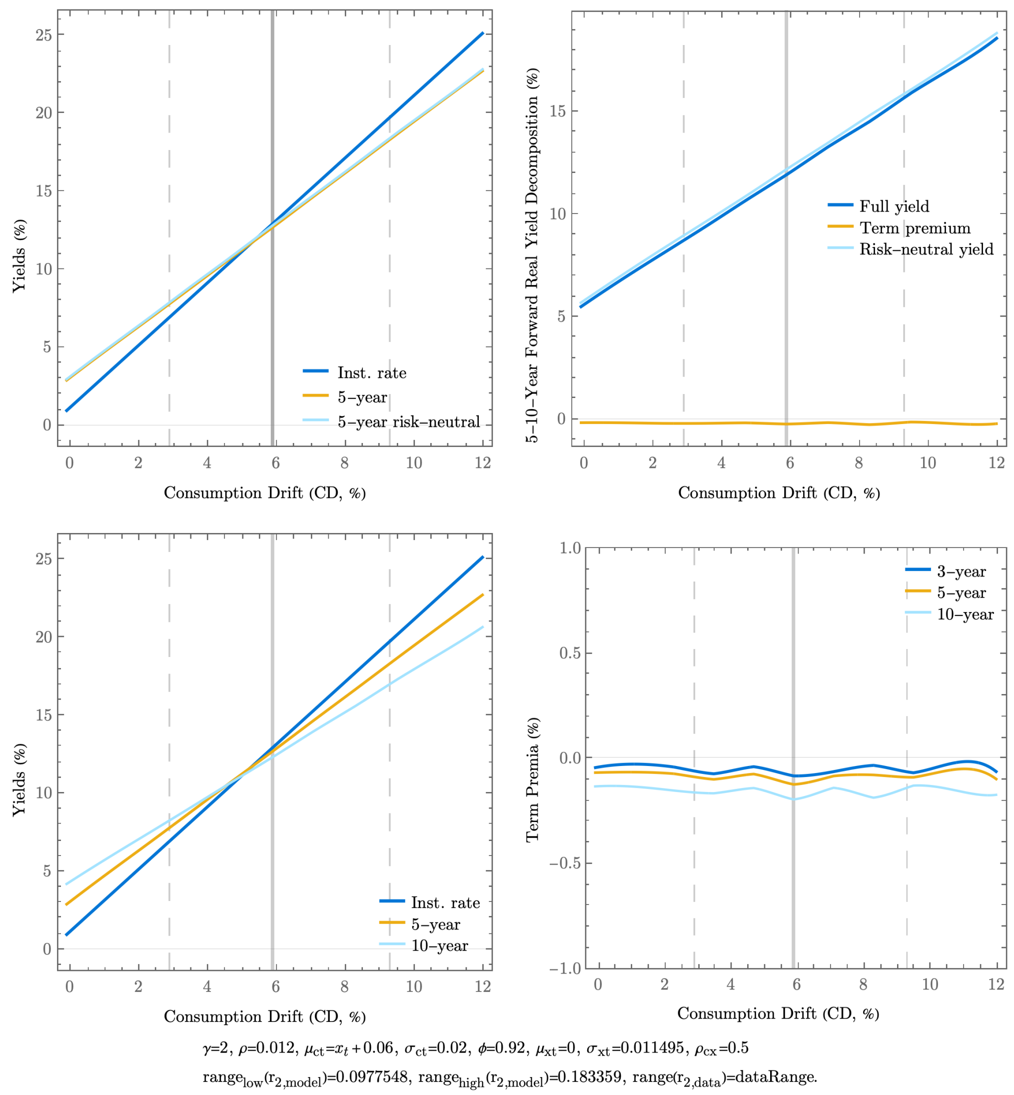

Figure IA.6: Time-varying and high CD with TSU. See Figure IA.1 for plot details.

IA.C.8 TSU-CD-HCV, $\sigma_{ct} = 0.16$

Yields shift down and term premia increase in absolute value but remain approximately constant.

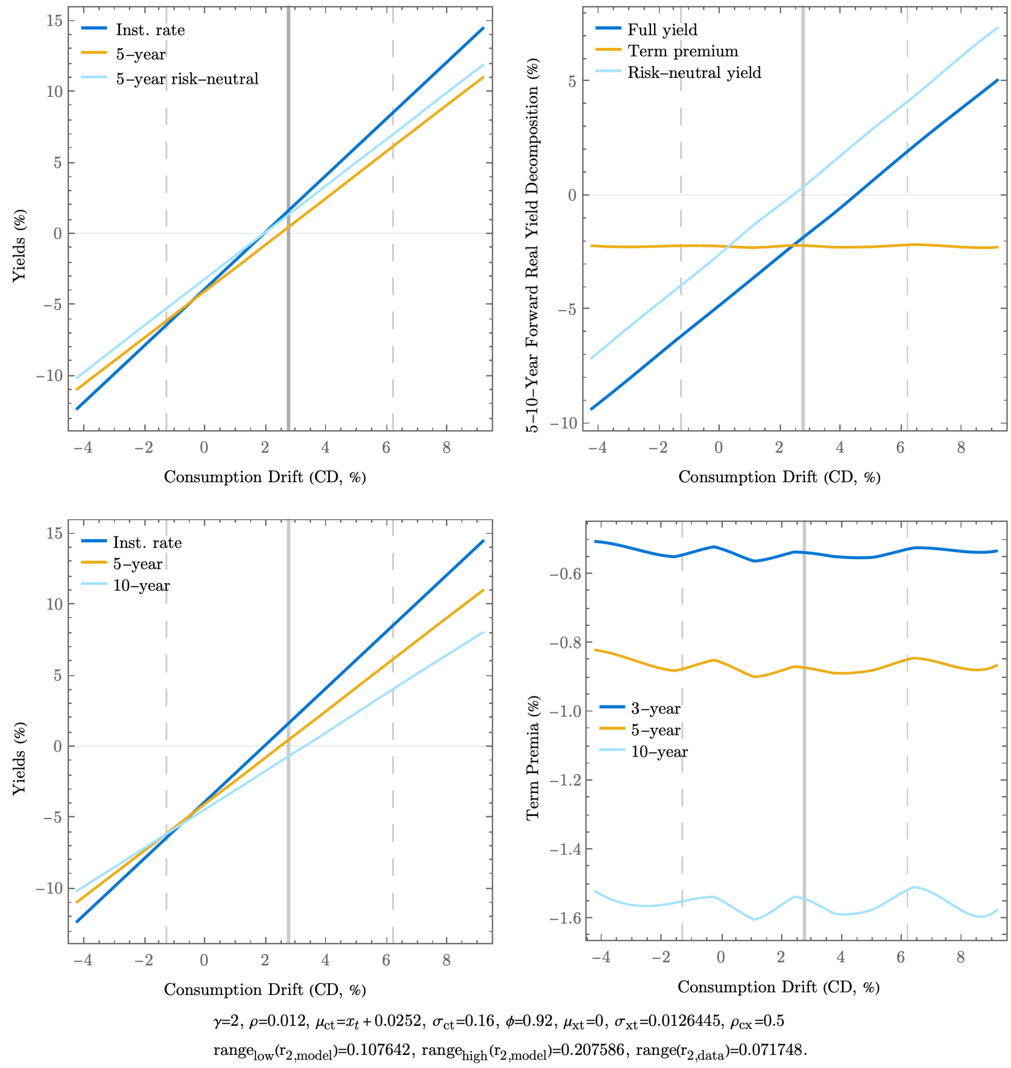

Figure IA.7: Time-varying CD with TSU and high CV. See Figure IA.1 for plot details.

IA.C.9 TSU-CV (baseline calibration used in main article)

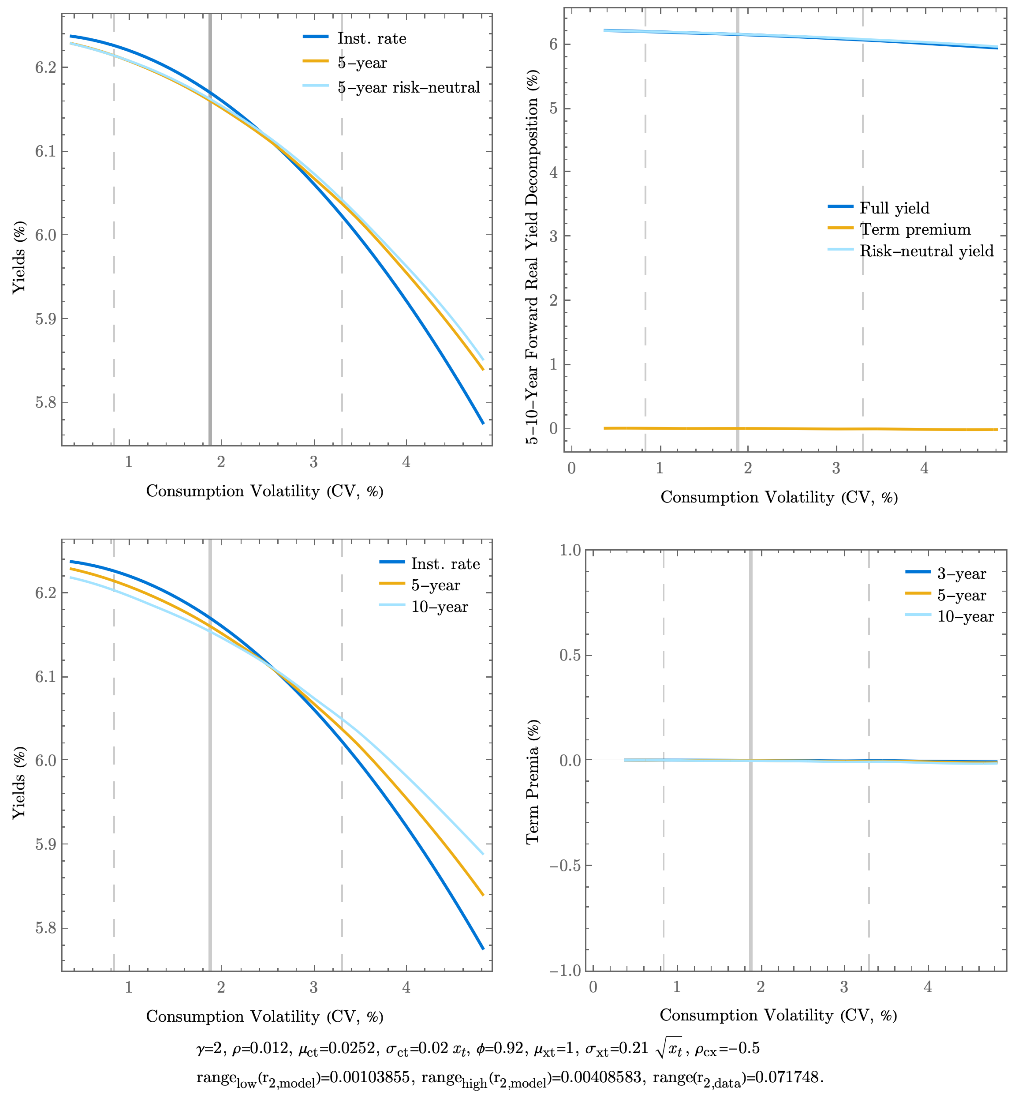

Figure IA.8: Time-varying CV with TSU. See Figure IA.1 for plot details.

IA.C.10 TSU-CV-HRA, $\gamma = 8$

Term premia increase in absolute value but not enough to turn positive, and yields become very high.

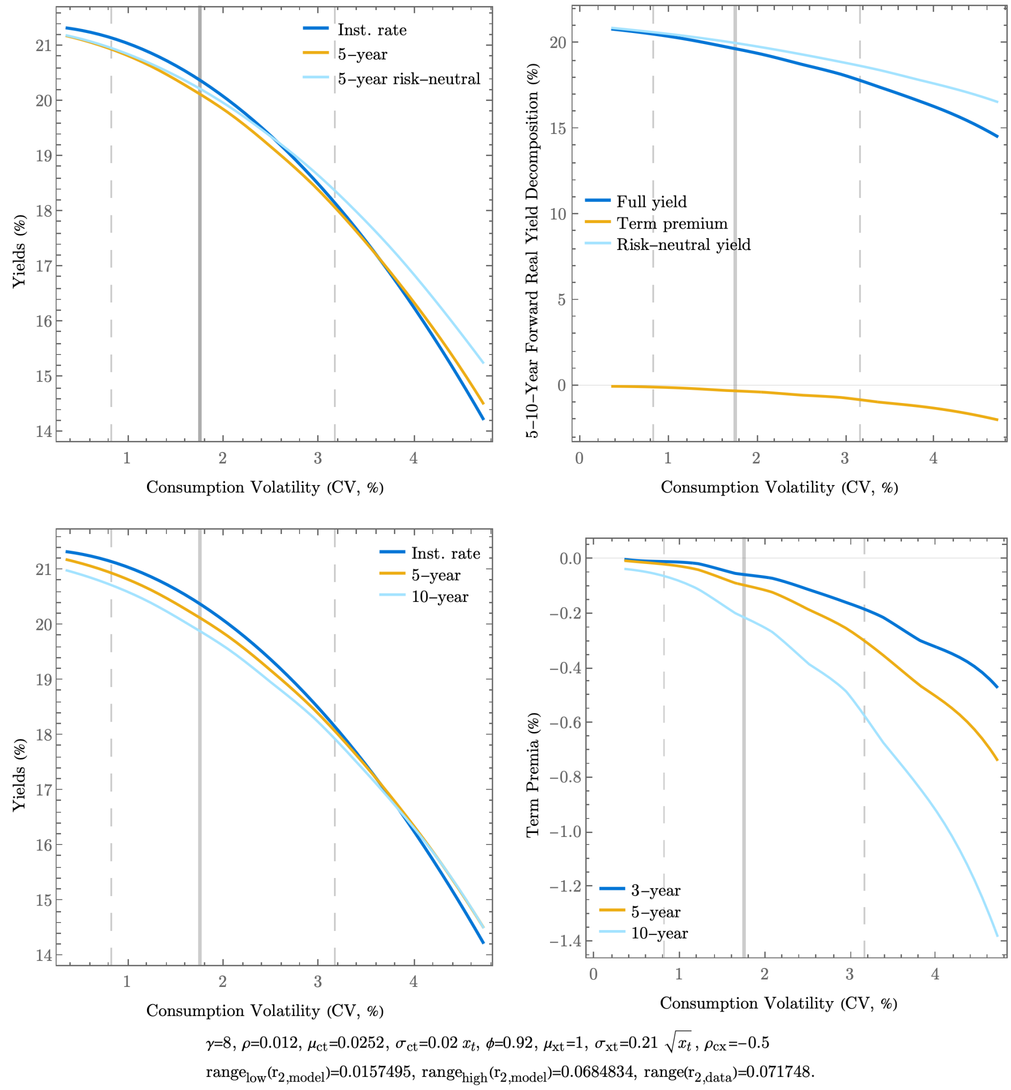

Figure IA.9: Time-varying CV with TSU and high risk aversion. See Figure IA.1 for plot details.

IA.C.11 TSU-CV-HCD, $\mu_{c0} = 0.08$

Term premia are unchanged but yields shift implausibly high.

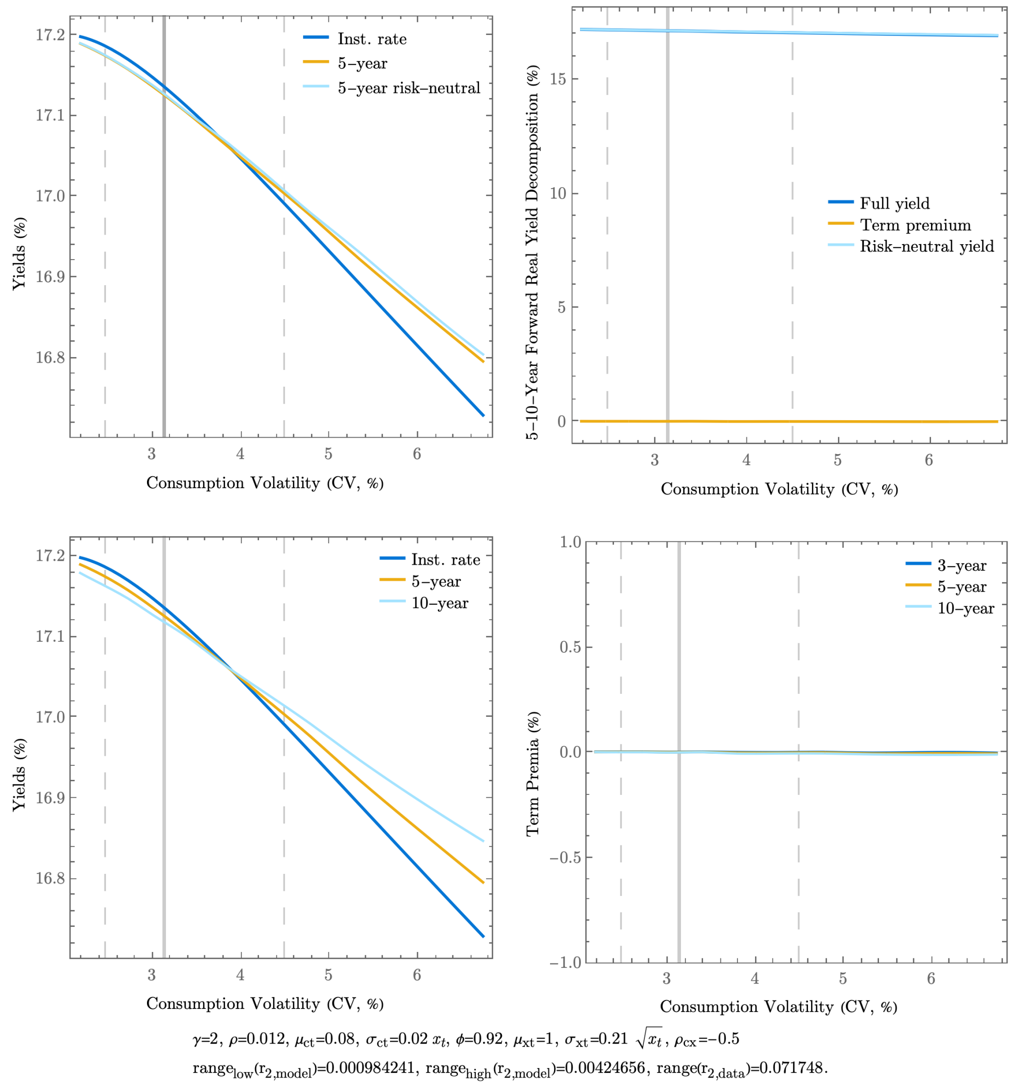

Figure IA.10: Time-varying CV with TSU and high CD. See Figure IA.1 for plot details.

IA.C.12 TSU-HCV (baseline calibration used in main article)

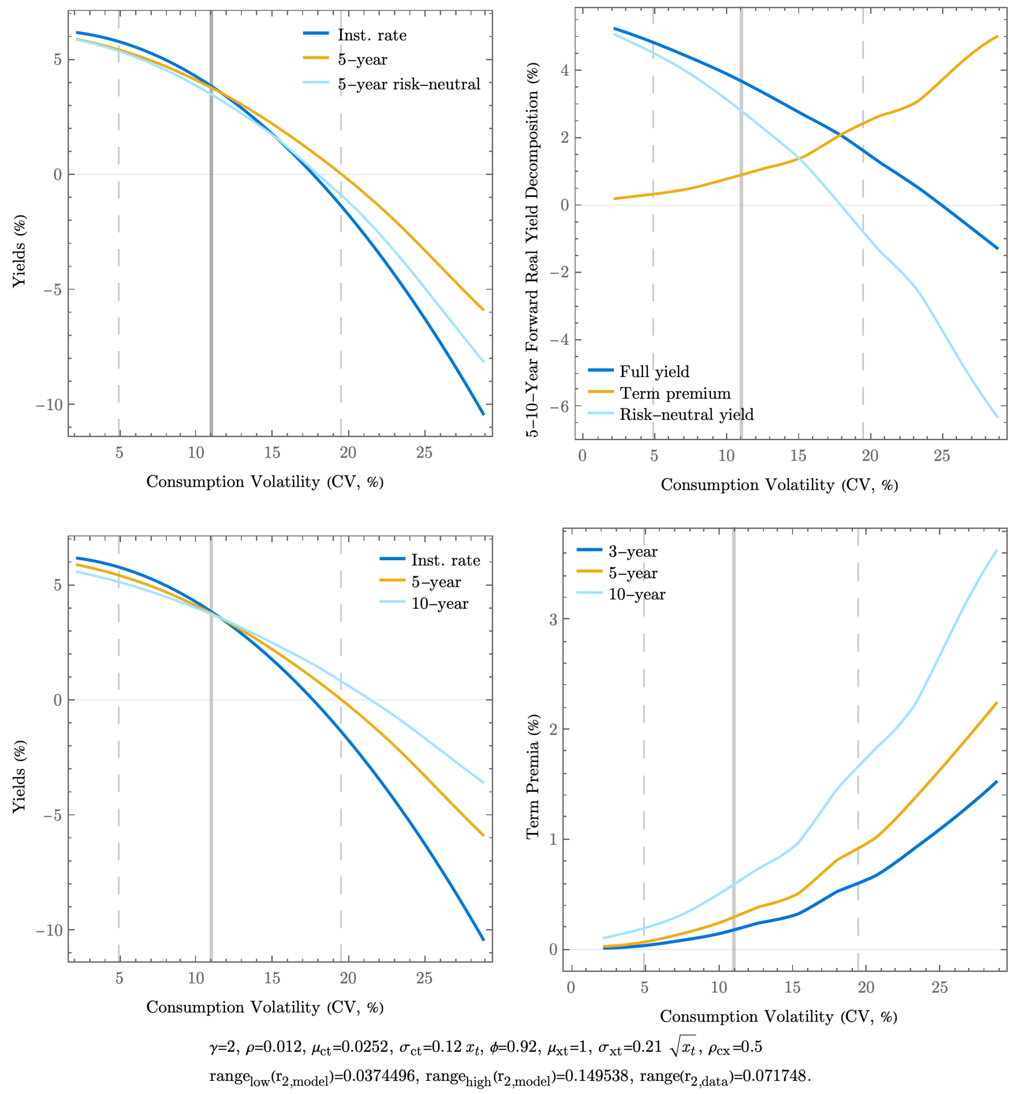

Figure IA.11: Time-varying and HCV with TSU and positive ρ_{cx}. See Figure IA.1 for plot details.

IA.C.13 TSU-HCV-NCor, $\rho_{cx} < 0$

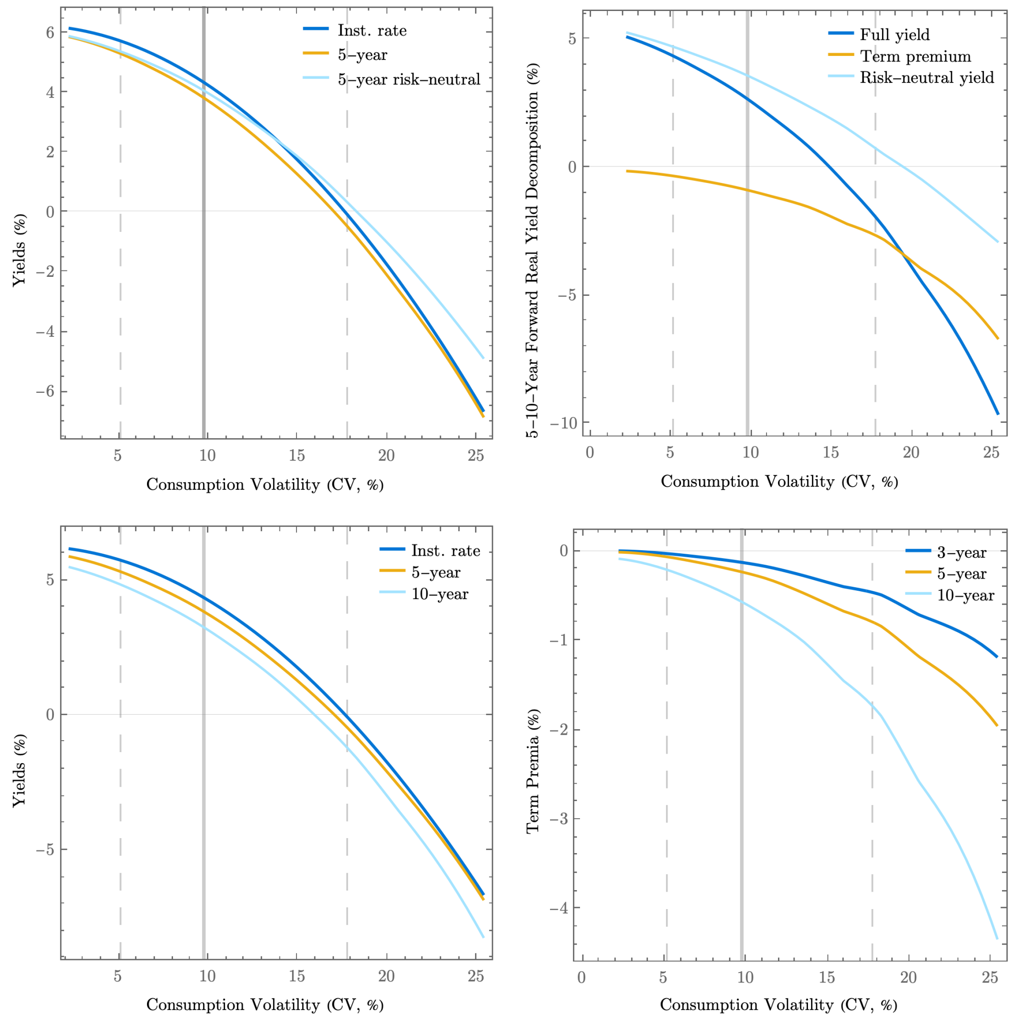

γ=2, ρ=0.012, μ_{ct}=0.0252, σ_{ct}=0.11 x_t, ϕ=0.92, μ_{xt}=1, σ_{xt}=0.2 $\sqrt{x_t}$, ρ_{cx}=−0.5

range$_{low}$($r_{2,model}$)=0.0306062, range$_{high}$($r_{2,model}$)=0.119326, range($r_{2,data}$)=0.071748.

Figure IA.12: Time-varying HCV with TSU and negative ρ_{cx}. See Figure IA.1 for plot details.

IA.C.14 Arb-DP (baseline calibration used in main article)

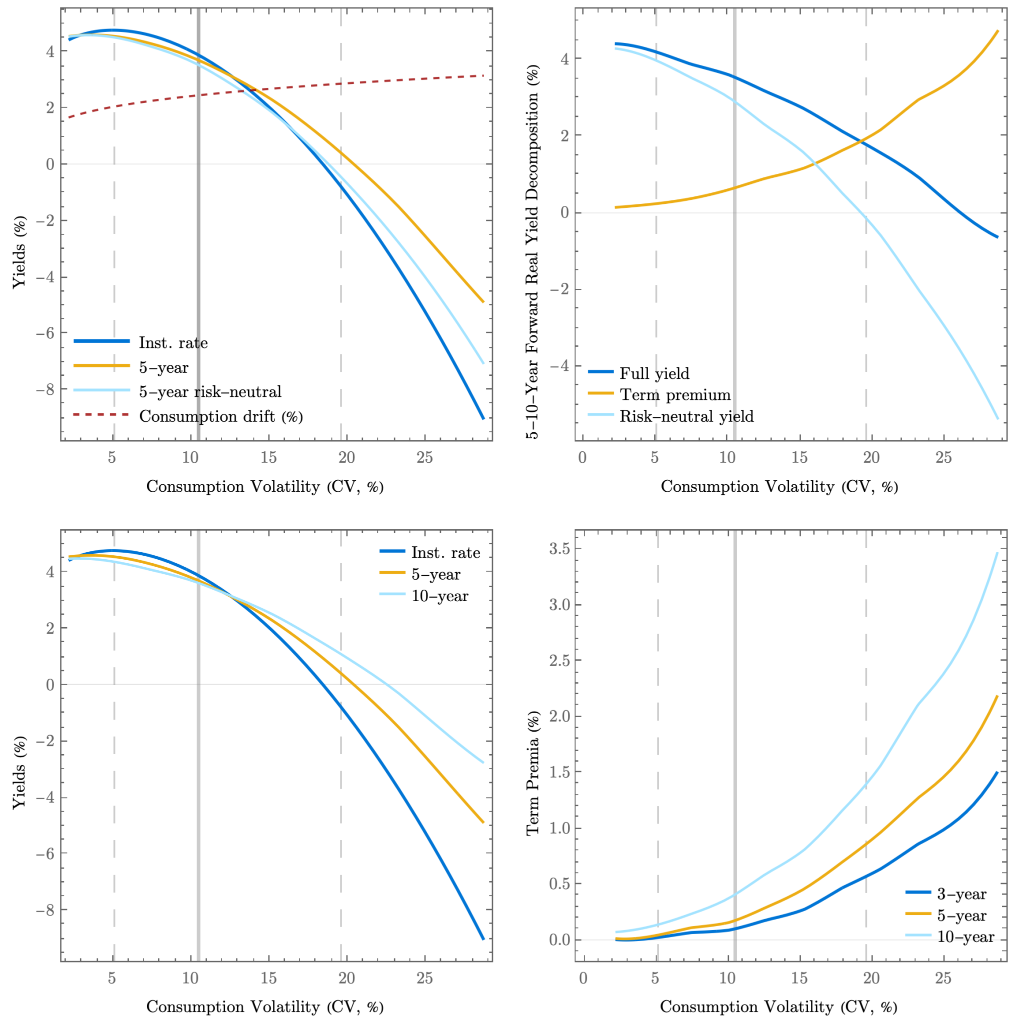

γ=2, ρ=0.012, μ_{ct}=0.0252 $\sqrt[4]{x_t}$, σ_{ct}=0.12 x_t, ϕ=0.92, μ_{xt}=1, σ_{xt}=0.21 $\sqrt{x_t}$, ρ_{cx}=0.5

range$_{\mathrm{low}}$(r$_{2,\mathrm{model}}$)=0.0222875, range$_{\mathrm{high}}$(r$_{2,\mathrm{model}}$)=0.132065, range(r$_{2,\mathrm{data}}$)=0.071748.

Figure IA.13: Both time-varying CD and CV with TSU, short-term rate decreasing in CV and positive ρ_{cx}. See Figure IA.1 for plot details.

IA.C.15 Arb-IN (baseline calibration used in main article)

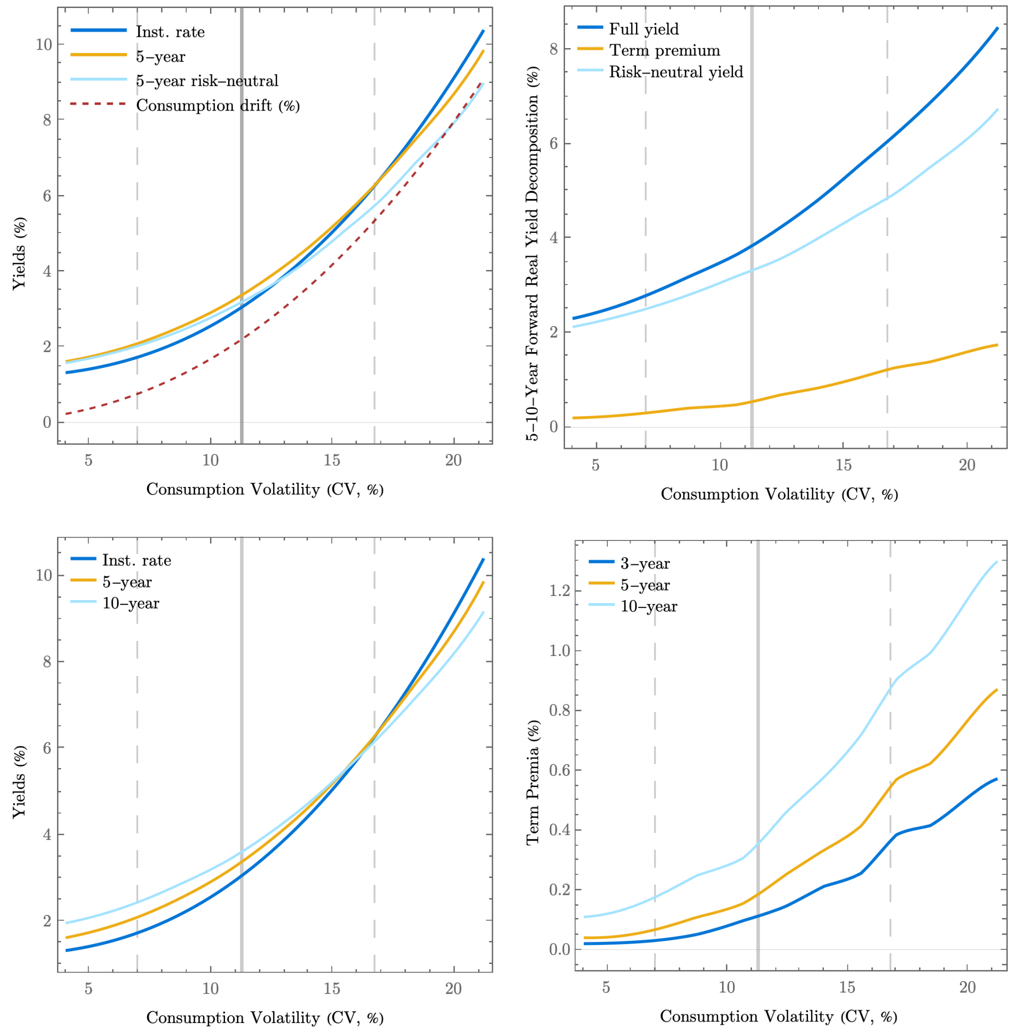

γ=2, ρ=0.012, μ_{ct}=0.0252 $x_t^{3/2}$, σ_{ct}=0.12 $x_t^{2/3}$, ϕ=0.92, μ_{xt}=1, σ_{xt}=0.21 $\sqrt{x_t}$, ρ_{cx}=−0.5

range$_{\text{low}}$(r$_{2,\text{model}}$)=0.0258998, range$_{\text{high}}$(r$_{2,\text{model}}$)=0.0818517, range(r$_{2,\text{data}}$)=dataRange.

Figure IA.14: Both time-varying CD and CV with TSU, short-term rate increasing in CV and negative ρ_{cx}. See Figure IA.1 for plot details.

IA.C.16 Arb-DN

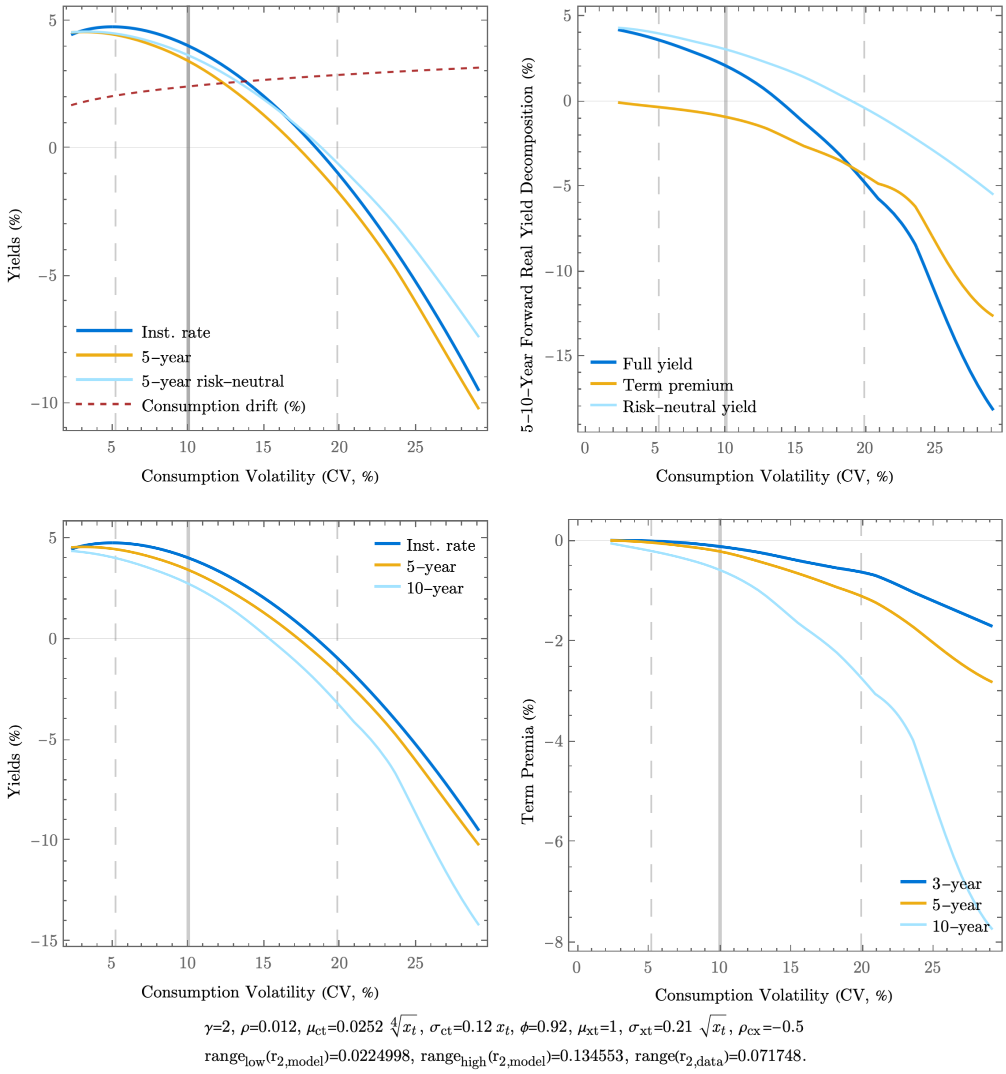

Figure IA.15: Both time-varying CD and CV with TSU, short-term rate decreasing in CV and negative ρ_{cx}. See Figure IA.1 for plot details.

IA.C.17 Arb-IP

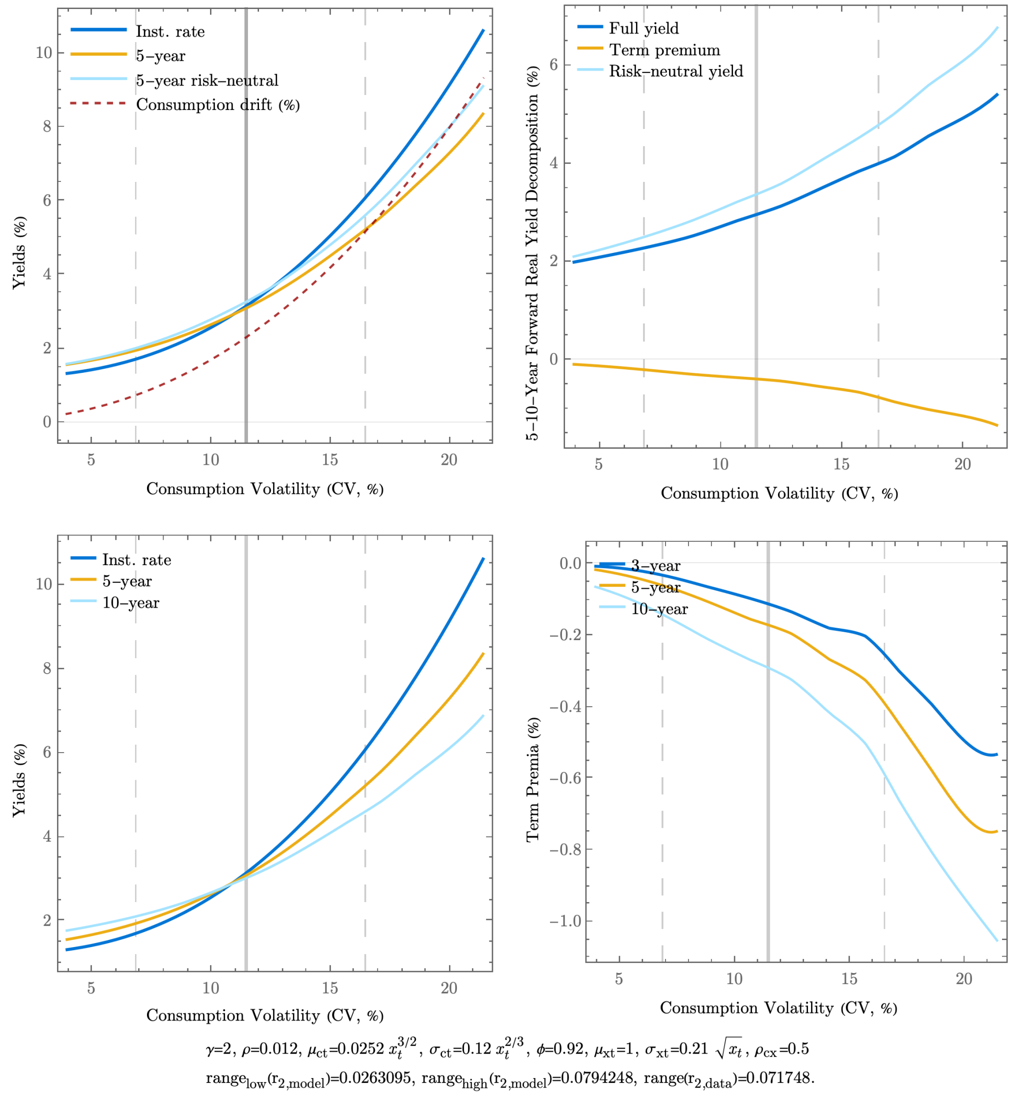

Figure IA.16: Both time-varying CD and CV with TSU, short-term rate increasing in CV and positive ρ_{cx}. See Figure IA.1 for plot details.

IA.C.18 TSU-Habit (baseline calibration used in main article)

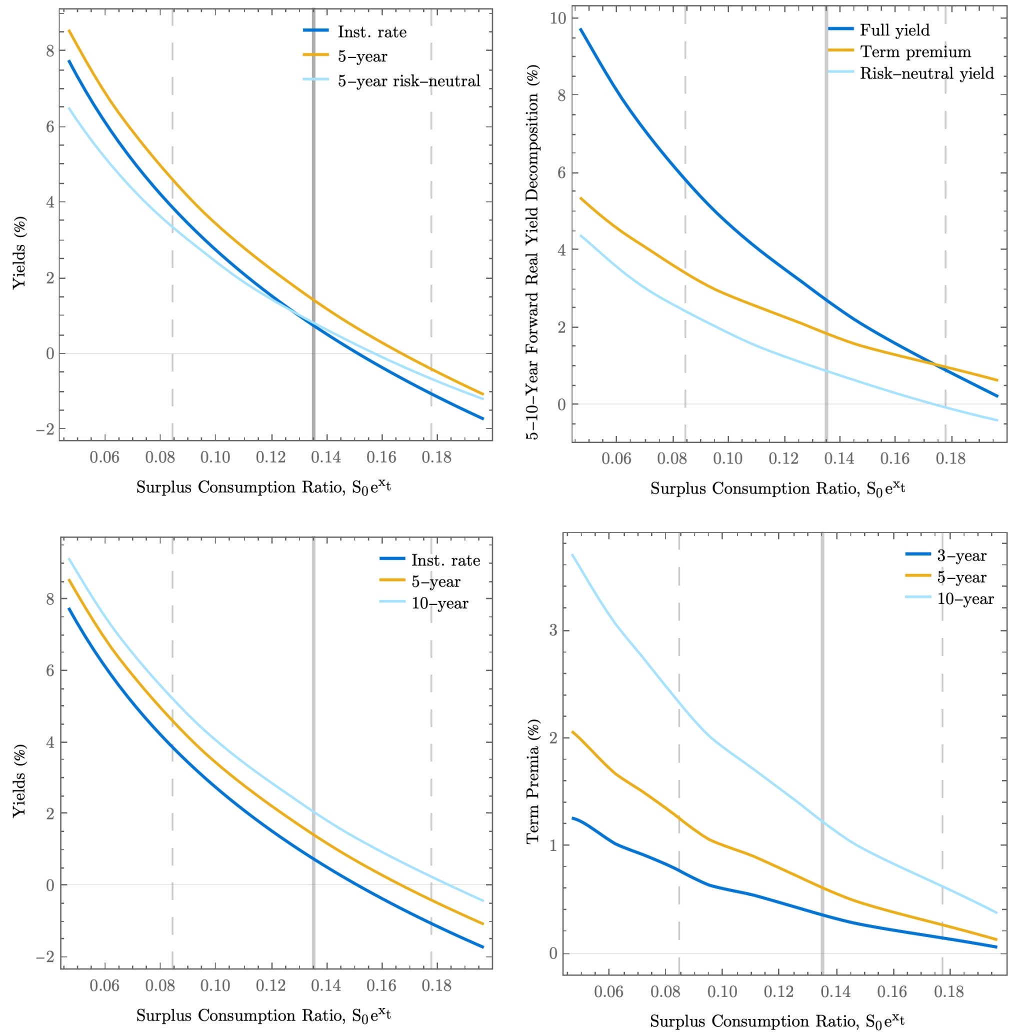

$\gamma=2$, $\rho=0.012$, $\mu_{ct}=0.0252$, $\sigma_{ct}=0.02$, $\phi=0.92$, $\mu_{xt}=0$, $\sigma_{xt}=0.02\,\mathrm{If}\left[x_t > 0.492061, 0, \dfrac{\sqrt{1-2\,x_t}}{0.02\sqrt{\dfrac{2}{-\frac{0.066}{2}-\log(0.92)}}}-1\right]$, $\rho_{cx}=1$

$\mathrm{range}_{low}(r_{2,model})=0.0323706$, $\mathrm{range}_{high}(r_{2,model})=0.0831215$, $\mathrm{range}(r_{2,data})=\mathrm{dataRange}$.

Figure IA.17: Time-varying external habit with TSU. See Figure IA.1 for plot details.

IA.C.19 TSU-Habit-Low.b, $b = 0.033$

Term premia are unchanged but yields become flatter.

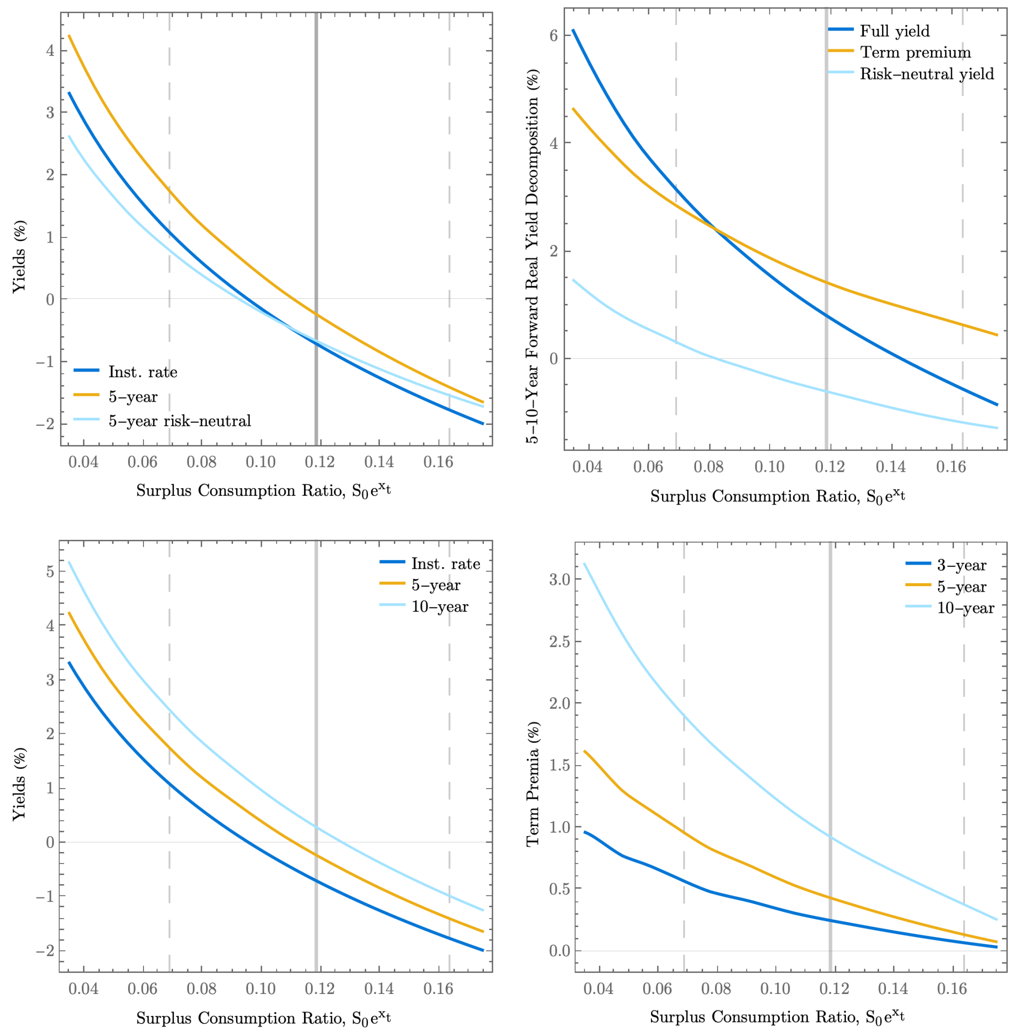

γ=2, ρ=0.012, μ_{ct}=0.0252, σ_{ct}=0.02, ϕ=0.92, μ_{xt}=0, $\sigma_{\mathrm{xt}}=0.02\,\mathrm{If}\left[x_t > 0.494019, 0, \frac{\sqrt{1-2\,x_t}}{0.02\sqrt{\frac{2}{-\frac{0.033}{2}-\log(0.92)}}}-1\right]$, ρ_{cx}=1

$\mathrm{range}_{\mathrm{low}}(\mathrm{r}_{2,\mathrm{model}})$=0.0181377, $\mathrm{range}_{\mathrm{high}}(\mathrm{r}_{2,\mathrm{model}})$=0.0475884, $\mathrm{range}(\mathrm{r}_{2,\mathrm{data}})$=dataRange.

Figure IA.18: Time-varying external habit with TSU and low b. See Figure IA.1 for plot details.

IA.C.20 TSU-Habit-Neg.b, $b = -0.033$

The short-term rate is now procyclical and term premia are negative.

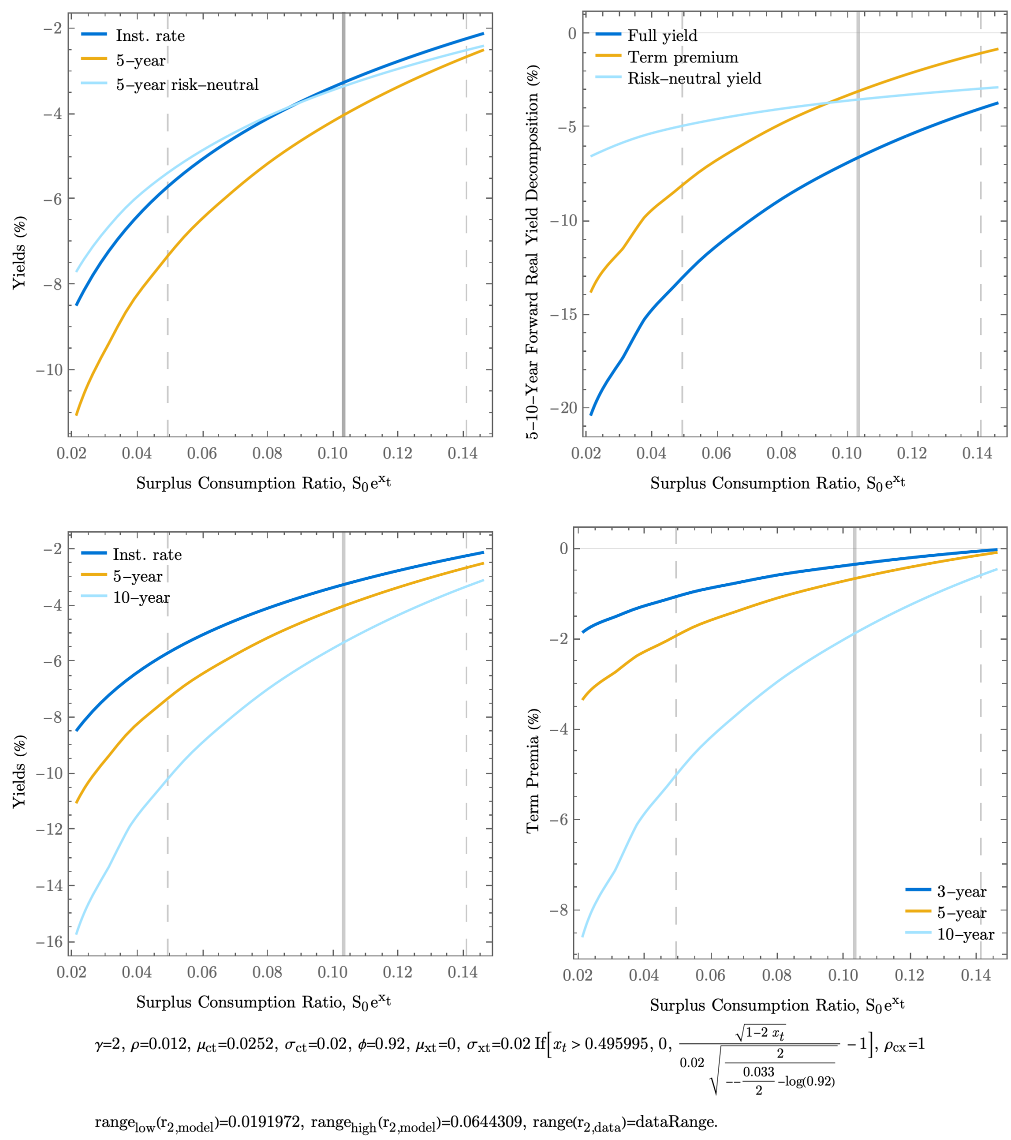

Figure IA.19: Time-varying external habit with TSU and $b < 0$. See Figure IA.1 for plot details.

IA.C.21 TSU-Habit-CSV, $\sigma_{xt} = \lambda(0)\sigma_{c0}$

Term premia become constant, since consumption volatility is constant in the habit model and state-variable heteroskedasticity is the only remaining source of time variation.

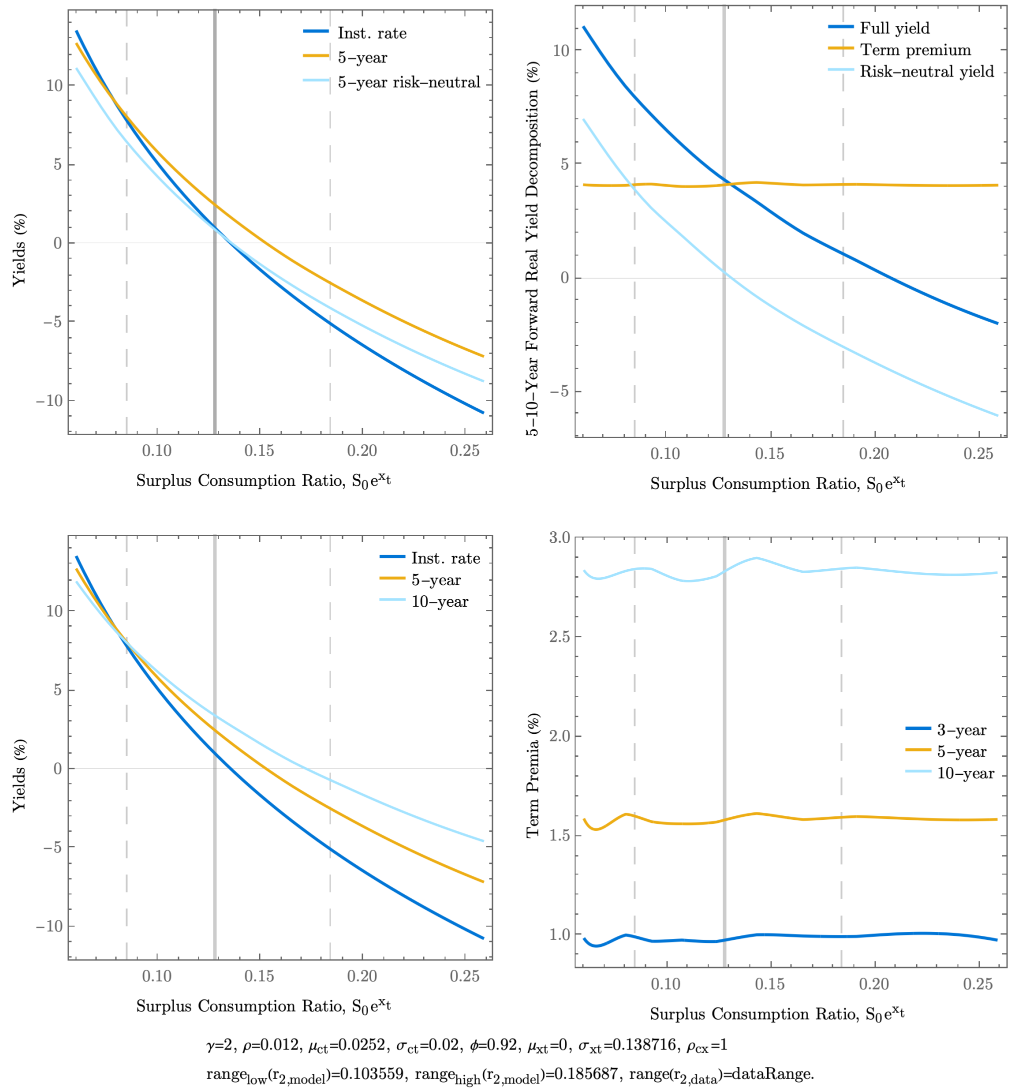

Figure IA.20: Time-varying external habit with TSU and constant state variable volatility. See Figure IA.1 for plot details.

IA.C.22 RU-CD (baseline calibration used in main article)

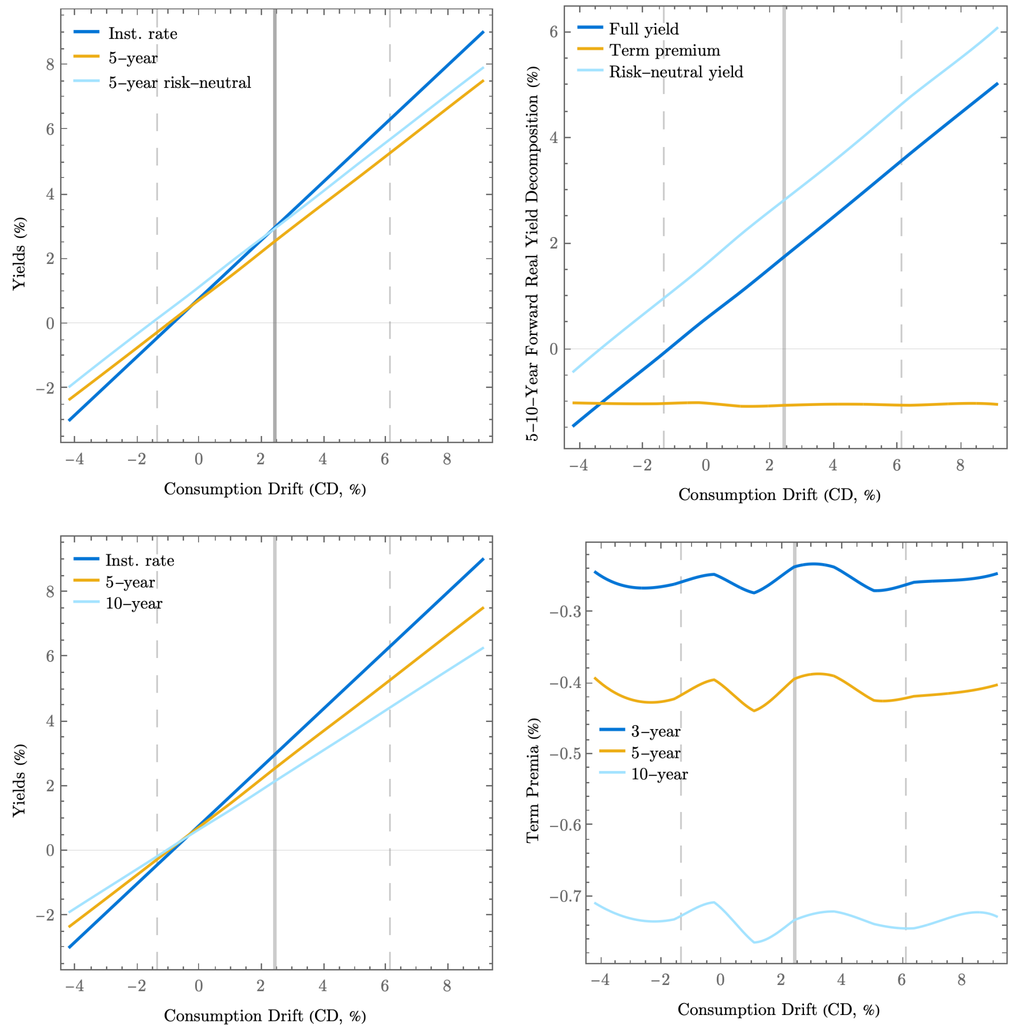

γ=2, ρ=0.012, $\mu_{\rm ct}=x_t+0.0252$, $\sigma_{\rm ct}$=0.02, ϕ=0.92, $\mu_{\rm xt}$=0, $\sigma_{\rm xt}$=0.0126445, $\rho_{\rm cx}$=0.5, ψ=1.11, approx. order=8
$\text{range}_{\text{low}}(\text{r}_{2,\text{model}})$=0.050672, $\text{range}_{\text{high}}(\text{r}_{2,\text{model}})$=0.0927875, $\text{range}(\text{r}_{2,\text{data}})$=dataRange.

Figure IA.21: Time-varying CD with RU. See Figure IA.1 for plot details.

IA.C.23 RU-CD-HRA, $\gamma = 6$

Term premia remain constant and negative but become significantly larger in absolute value. This suggests that time-varying risk aversion would produce time-varying term premia — a mechanism similar to the habit model.

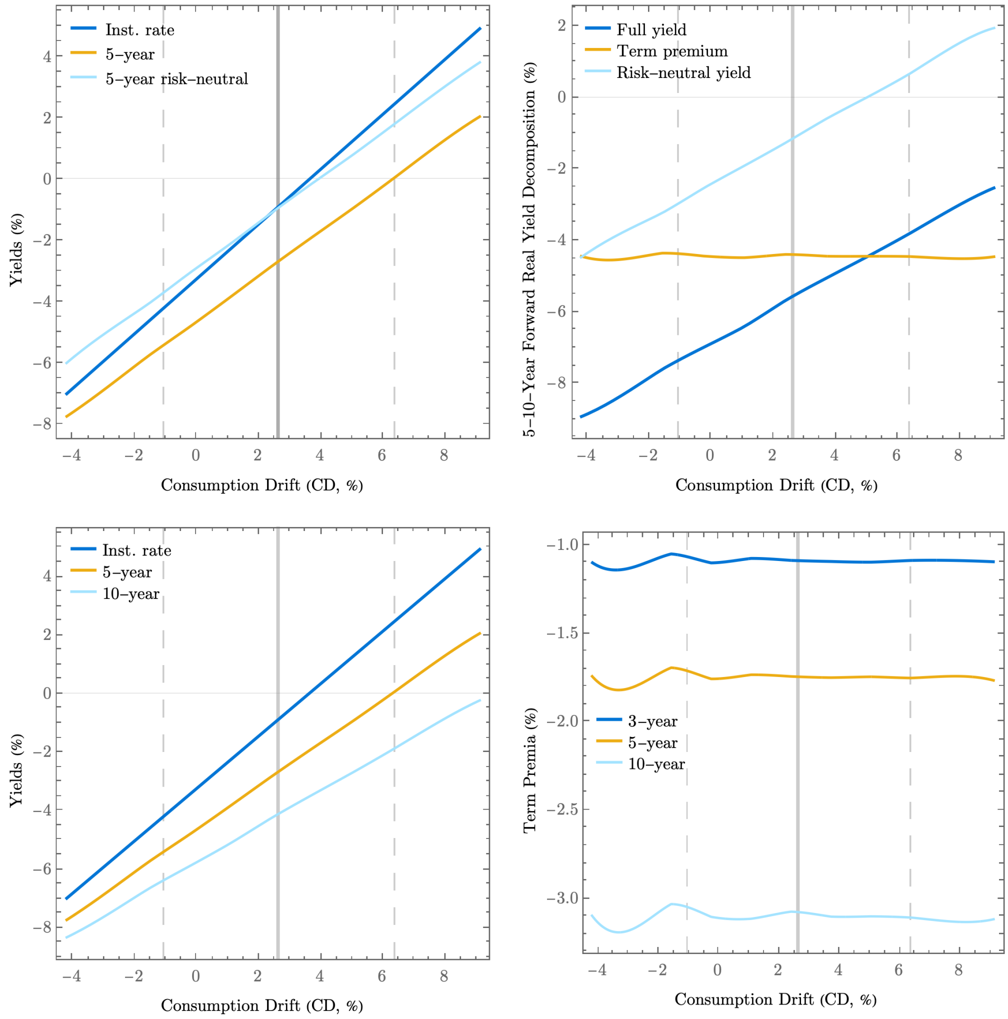

γ=6, ρ=0.012, μ_{ct}=x_t+0.0252, σ_{ct}=0.02, ϕ=0.92, μ_{xt}=0, σ_{xt}=0.0126445, ρ_{cx}=0.5, ψ=1.11, approx. order=8

$\mathrm{range_{low}}(\mathrm{r_{2,model}})$=0.0491264, $\mathrm{range_{high}}(\mathrm{r_{2,model}})$=0.0893581, $\mathrm{range}(\mathrm{r_{2,data}})$=0.071748.

Figure IA.22: Time-varying CD with RU and high risk aversion. See Figure IA.1 for plot details.

IA.C.24 RU-CD-HIES, $\psi = 1.43$

Term premia do not change significantly. The range of the short rate increases.

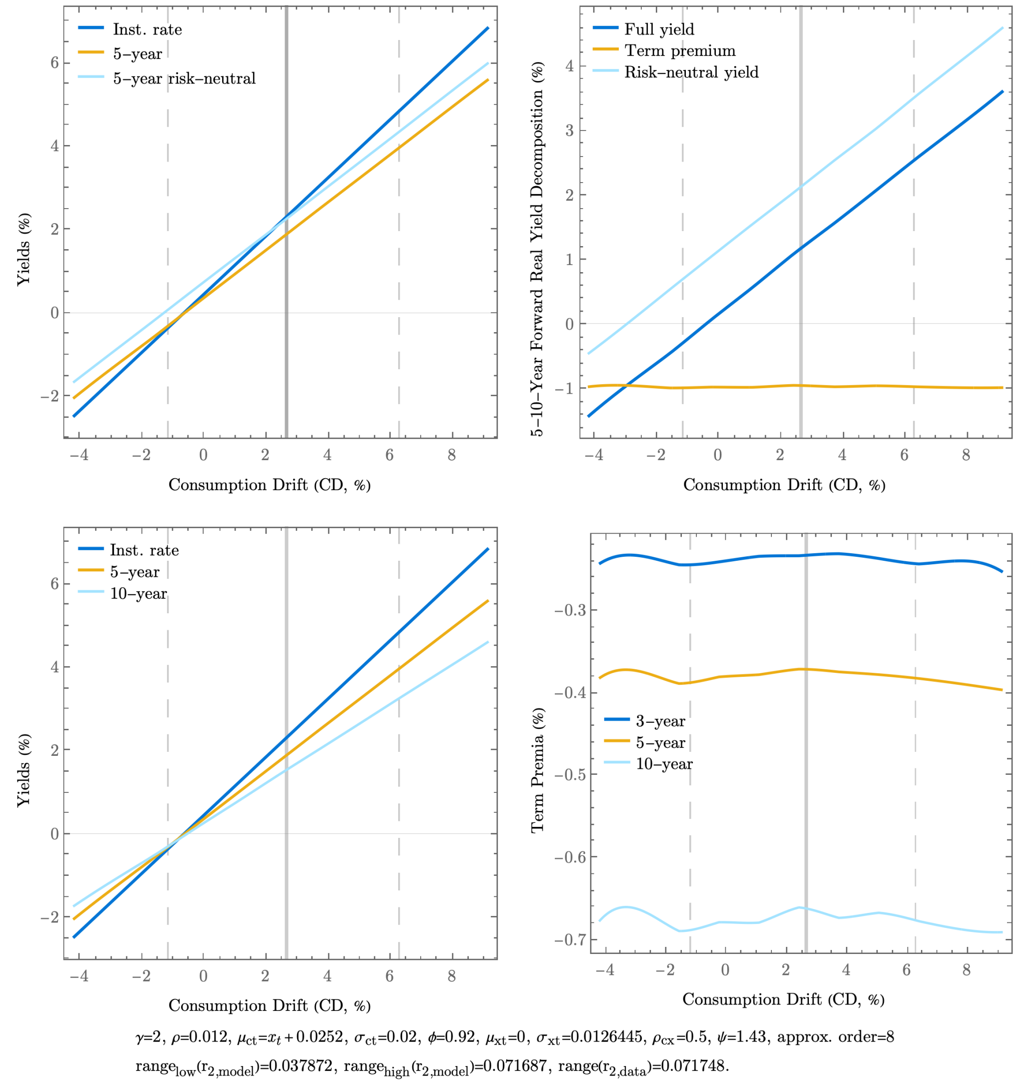

Figure IA.23: Time-varying CD with RU and high IES. See Figure IA.1 for plot details.

IA.C.25 RU-CD-LIES, $\psi = 0.83$

Term premia do not change significantly. Curiously the range of the short rate increases again.

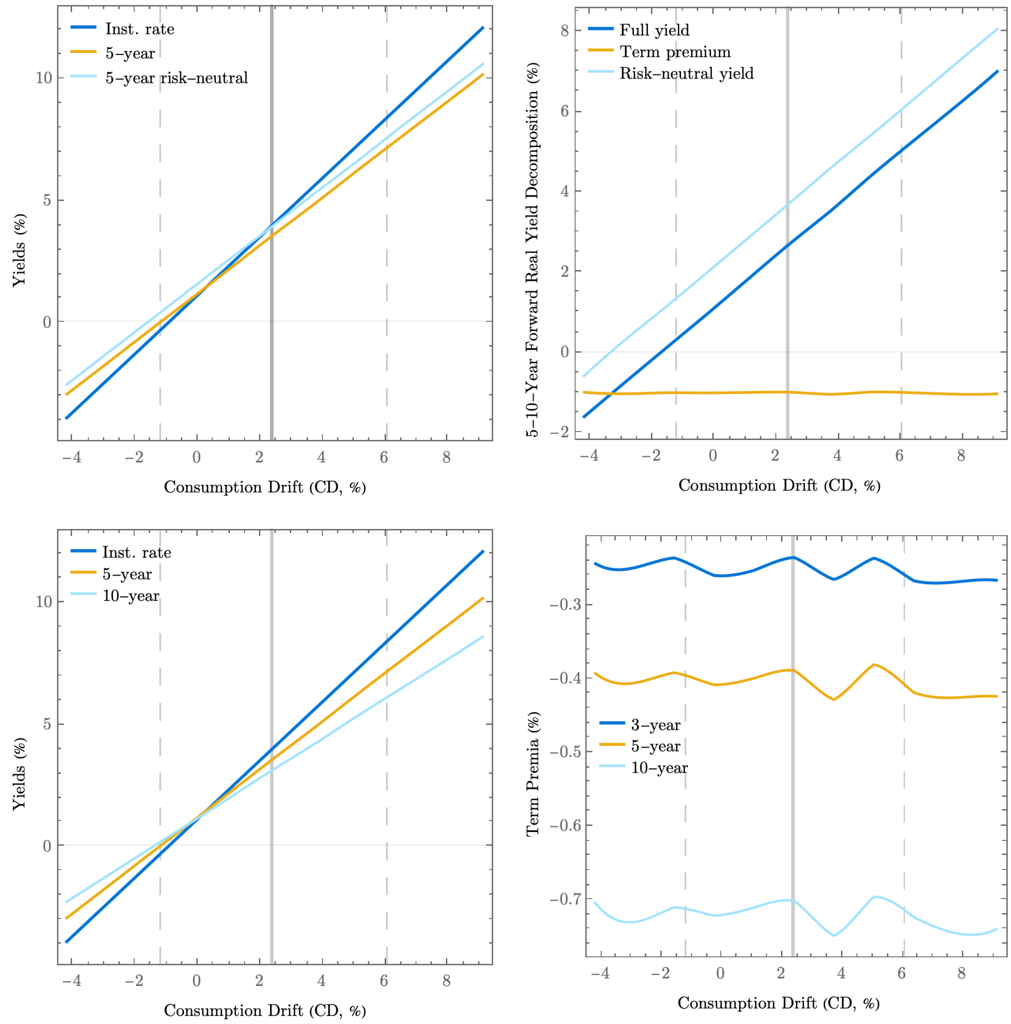

γ=2, ρ=0.012, μ_{ct}=x_t+0.0252, σ_{ct}=0.02, ϕ=0.92, μ_{xt}=0, σ_{xt}=0.0126445, ρ_{cx}=0.5, ψ=0.83, approx. order=11

$\mathrm{range}_{\mathrm{low}}(\mathrm{r}_{2,\mathrm{model}})$=0.0651376, $\mathrm{range}_{\mathrm{high}}(\mathrm{r}_{2,\mathrm{model}})$=0.121441, $\mathrm{range}(\mathrm{r}_{2,\mathrm{data}})$=0.071748.

Figure IA.24: Time-varying CD with RU and low IES. See Figure IA.1 for plot details.

IA.C.26 RU-CD-HCor, $\rho_{cx} = 1$

Term premia increase in absolute value but do not double in size as the correlation parameter does.

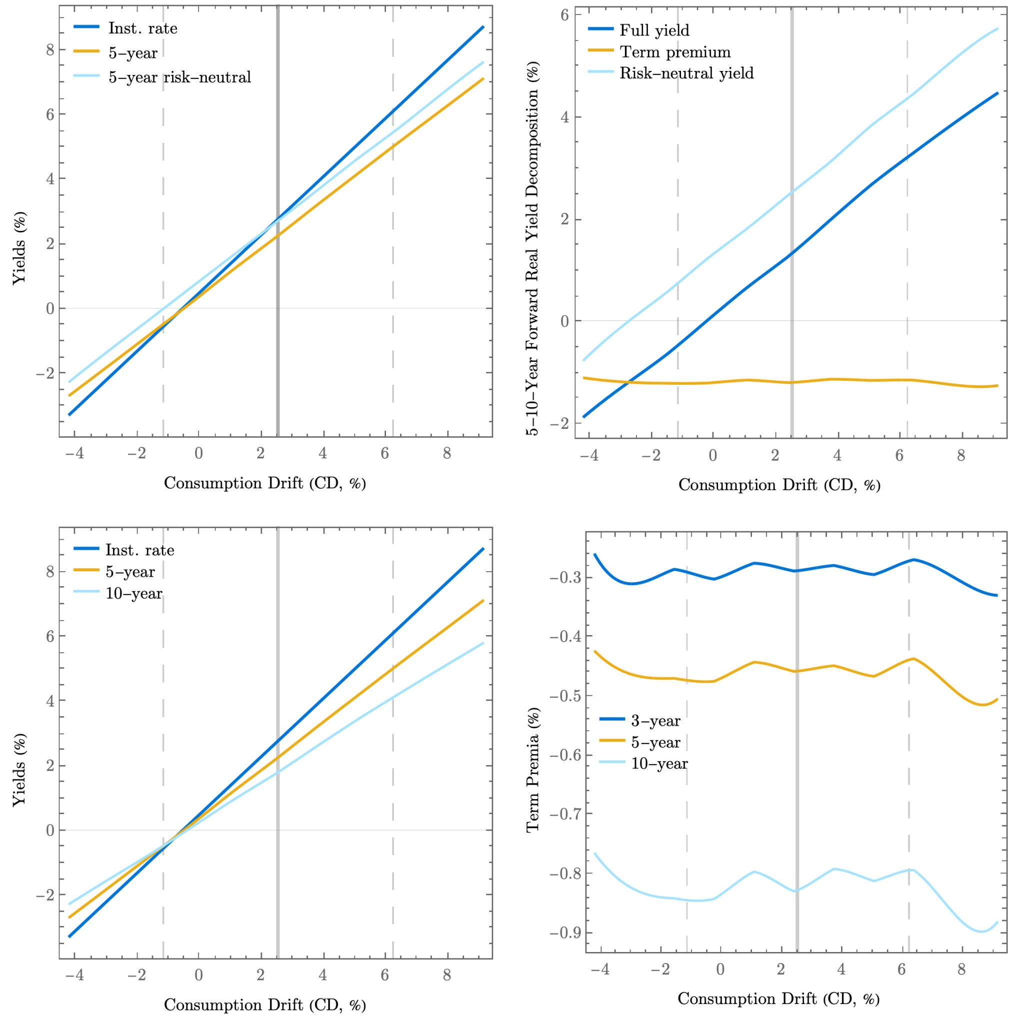

γ=2, ρ=0.012, μ_{ct}=x_t+0.0252, σ_{ct}=0.02, ϕ=0.92, μ_{xt}=0, σ_{xt}=0.0126445, ρ_{cx}=1, ψ=1.11, approx. order=8

range$_{low}$(r$_{2,model}$)=0.0506132, range$_{high}$(r$_{2,model}$)=0.0914971, range(r$_{2,data}$)=0.071748.

Figure IA.25: Time-varying CD with RU and high ρ_{cx}. See Figure IA.1 for plot details.

IA.C.27 RU-CD-NCor, $\rho_{cx} < 0$

Term premia increase but remain negative, as the dominant term in A does not involve ρ_{cx}.

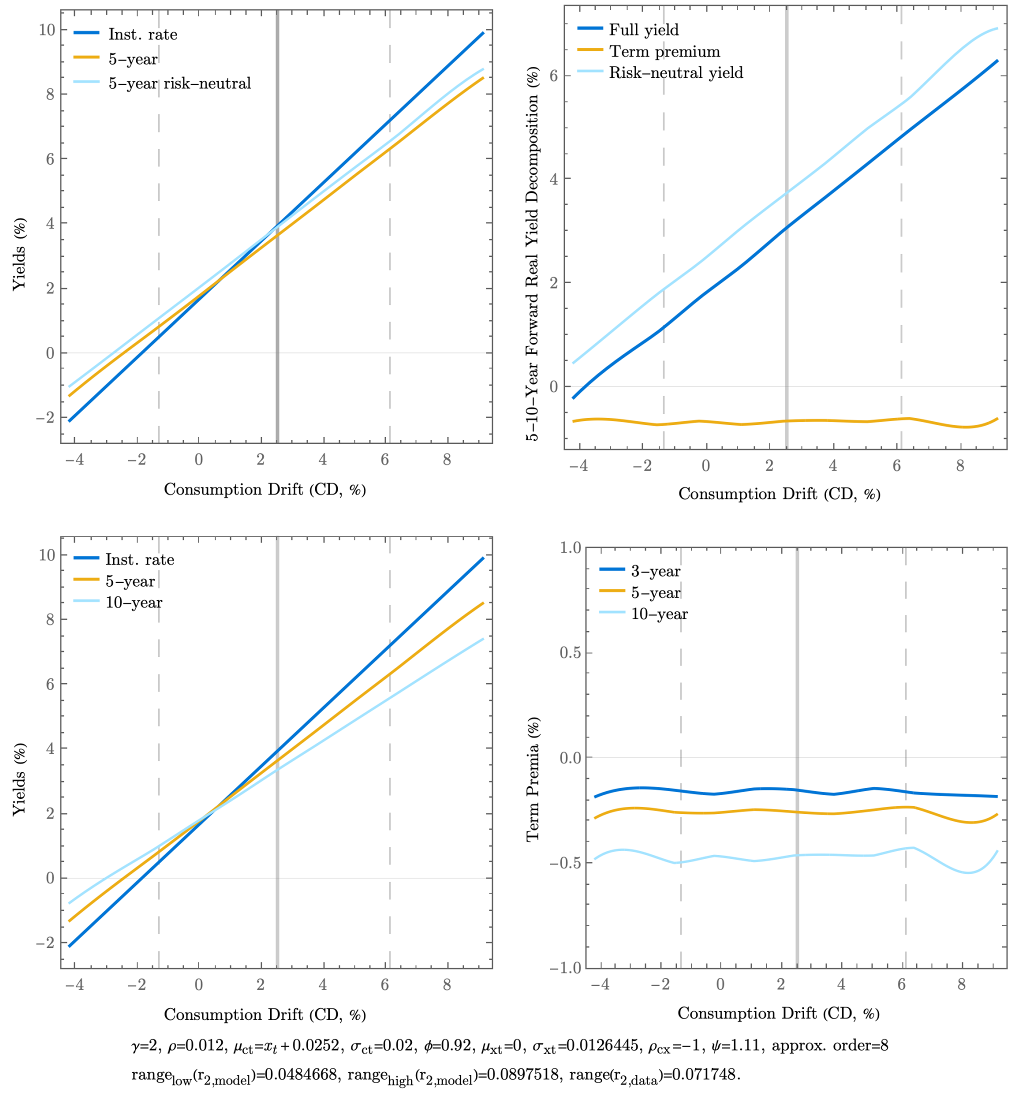

Figure IA.26: Time-varying CD with RU and negative ρ_{cx}. See Figure IA.1 for plot details.

IA.C.28 RU-HCD, $\mu_{x0} = 0.05$

Term premia are unchanged; yields increase.

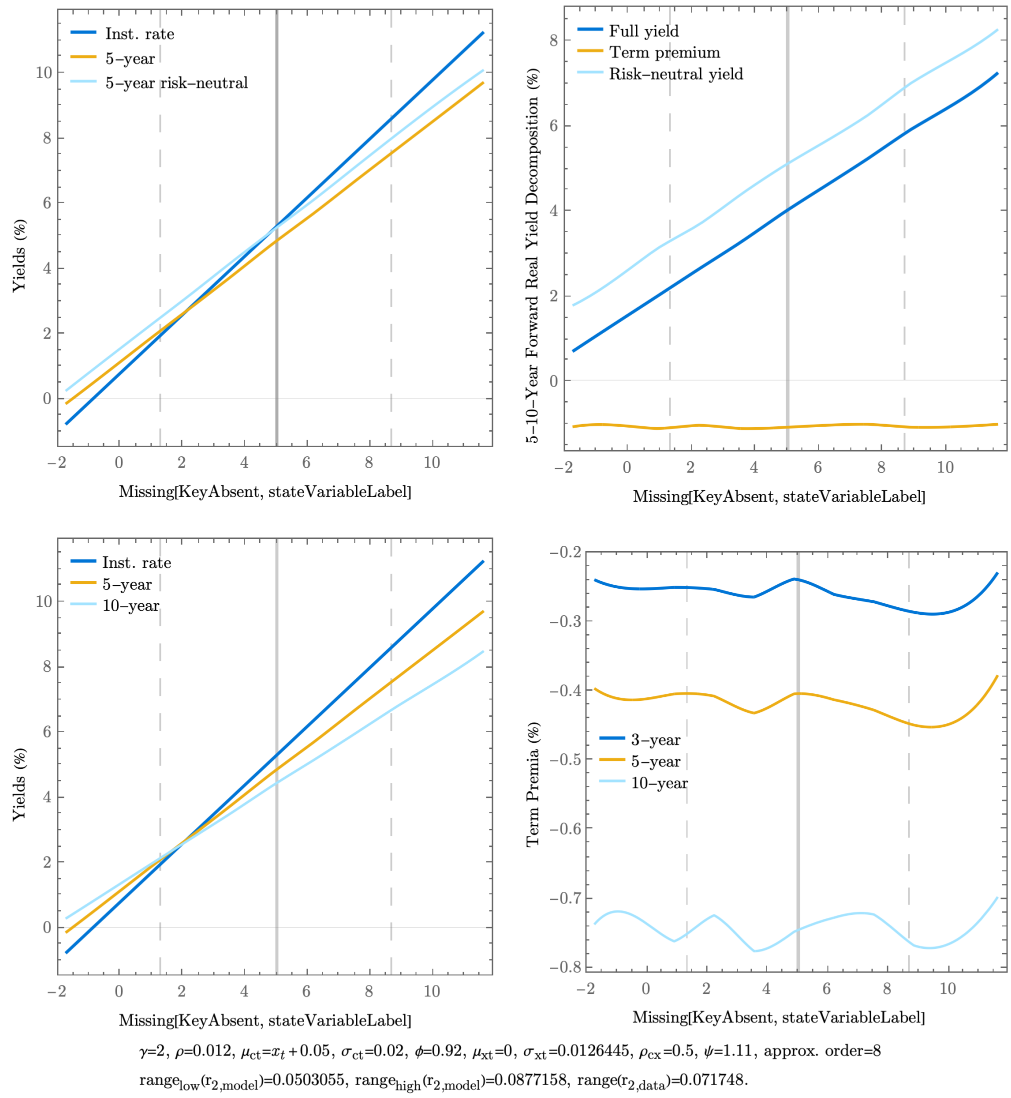

Figure IA.27: Time-varying and high CD with RU. See Figure IA.1 for plot details.

IA.C.29 RU-CD-HCV, $\sigma_{ct} = 0.08$

Term premia are unchanged; yields decrease.

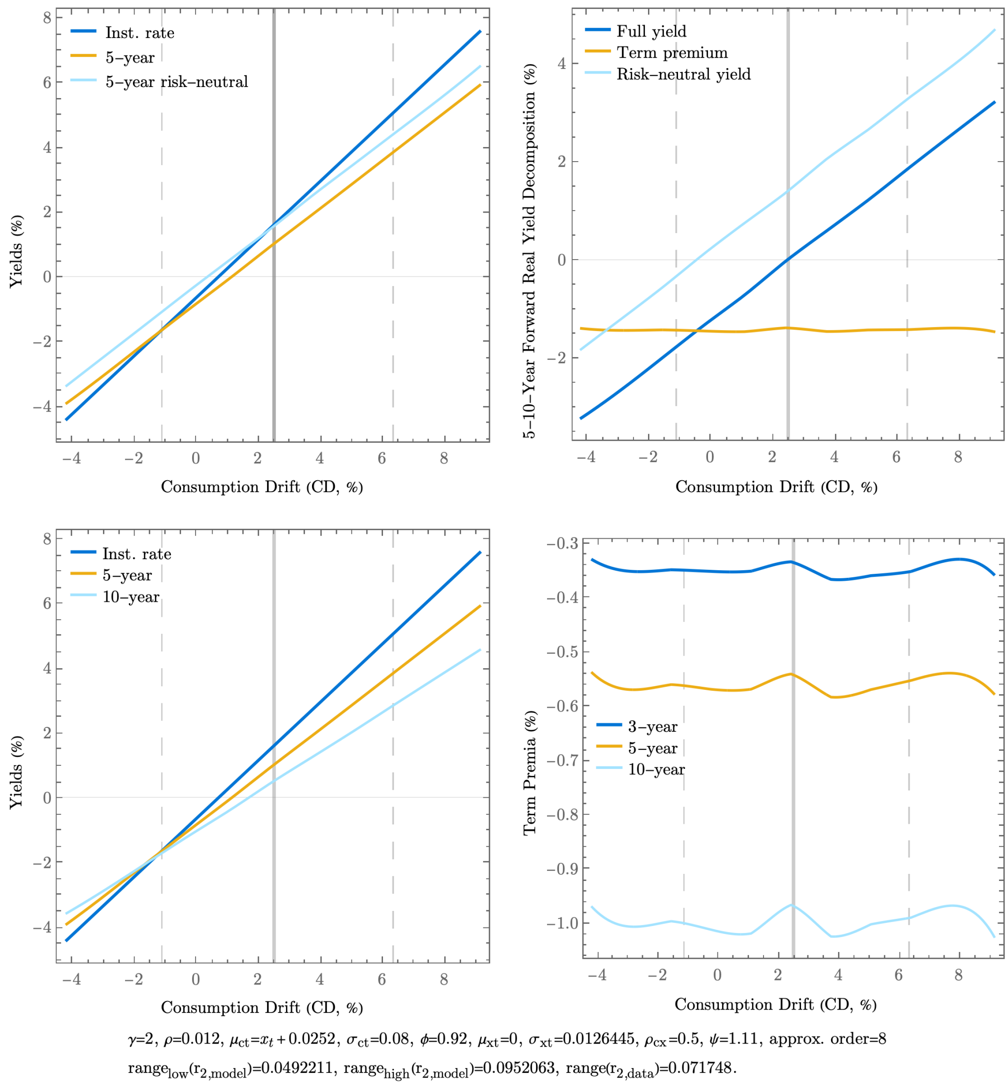

Figure IA.28: Time-varying CD with RU and high CV. See Figure IA.1 for plot details.

IA.C.30 RU-CD-Heterosk-PCor

When the state variable is heteroskedastic, term premia become time-varying. They remain negative here.

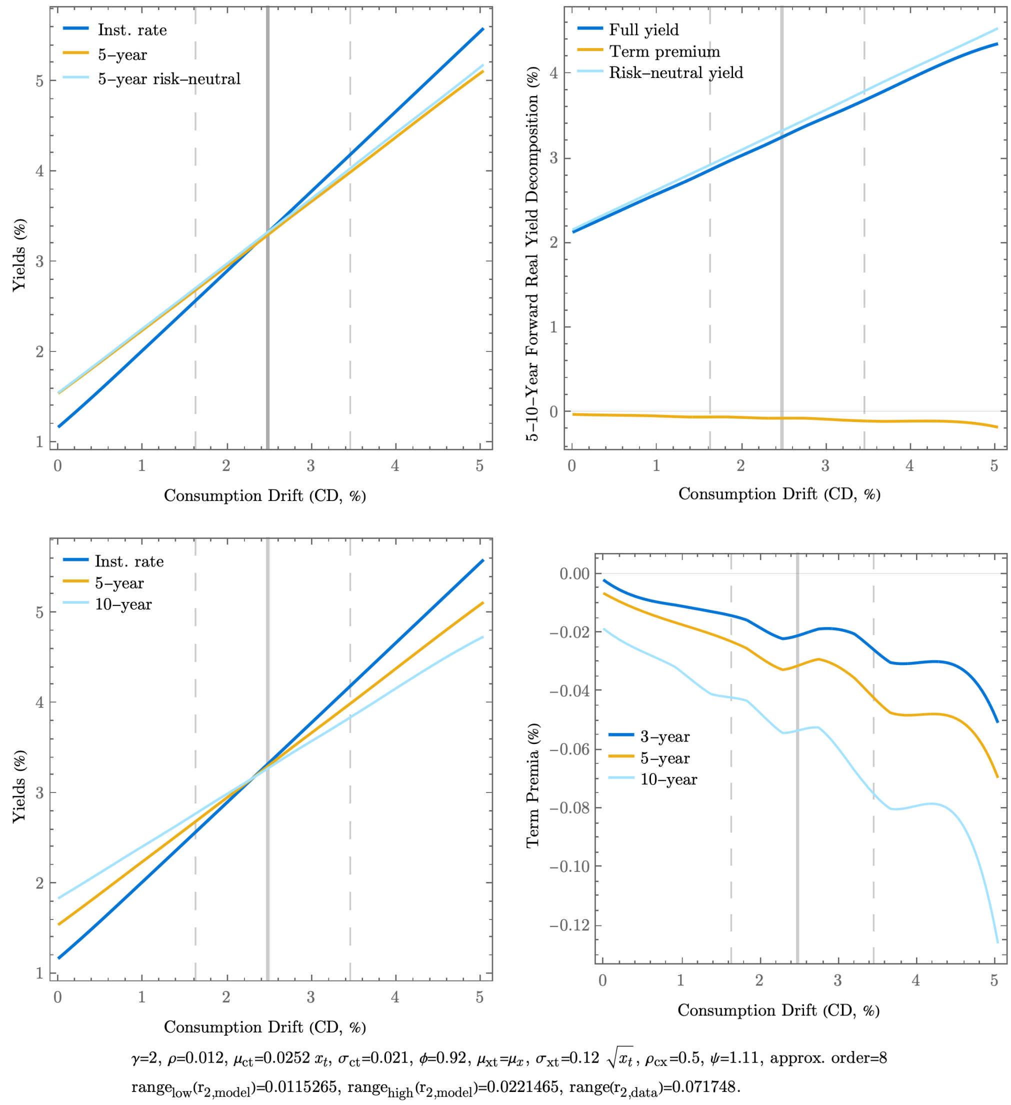

Figure IA.29: Time-varying and heteroskedastic CD with RU and positive ρ_{cx}. See Figure IA.1 for plot details.

IA.C.31 RU-CD-Heterosk-NCor

Despite the sign change in ρ_{cx}, term premia remain negative because the dominant component of A does not contain ρ_{cx}.

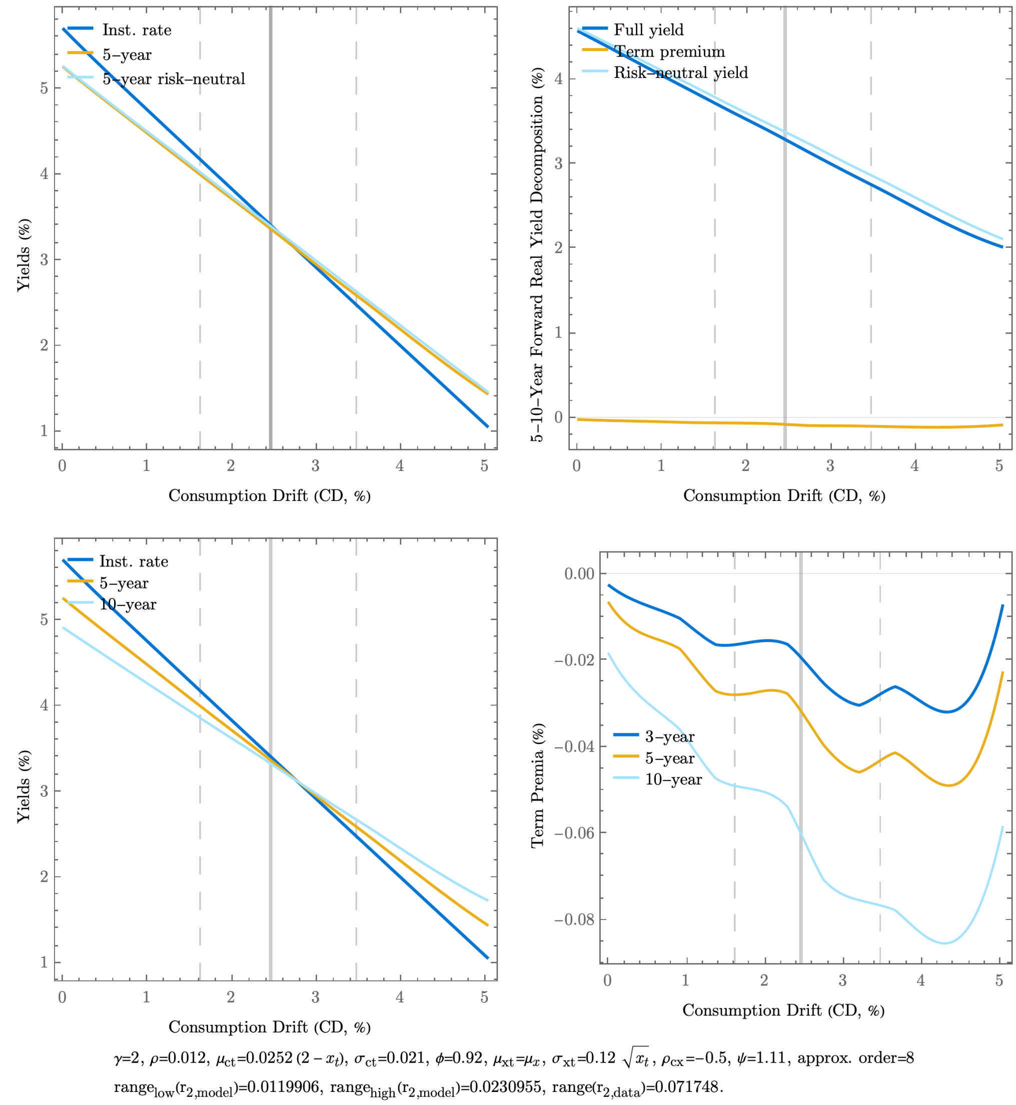

Figure IA.30: Time-varying and heteroskedastic CD with RU and negative ρ_{cx}. See Figure IA.1 for plot details.

IA.C.32 RU-CV (baseline calibration used in main article)

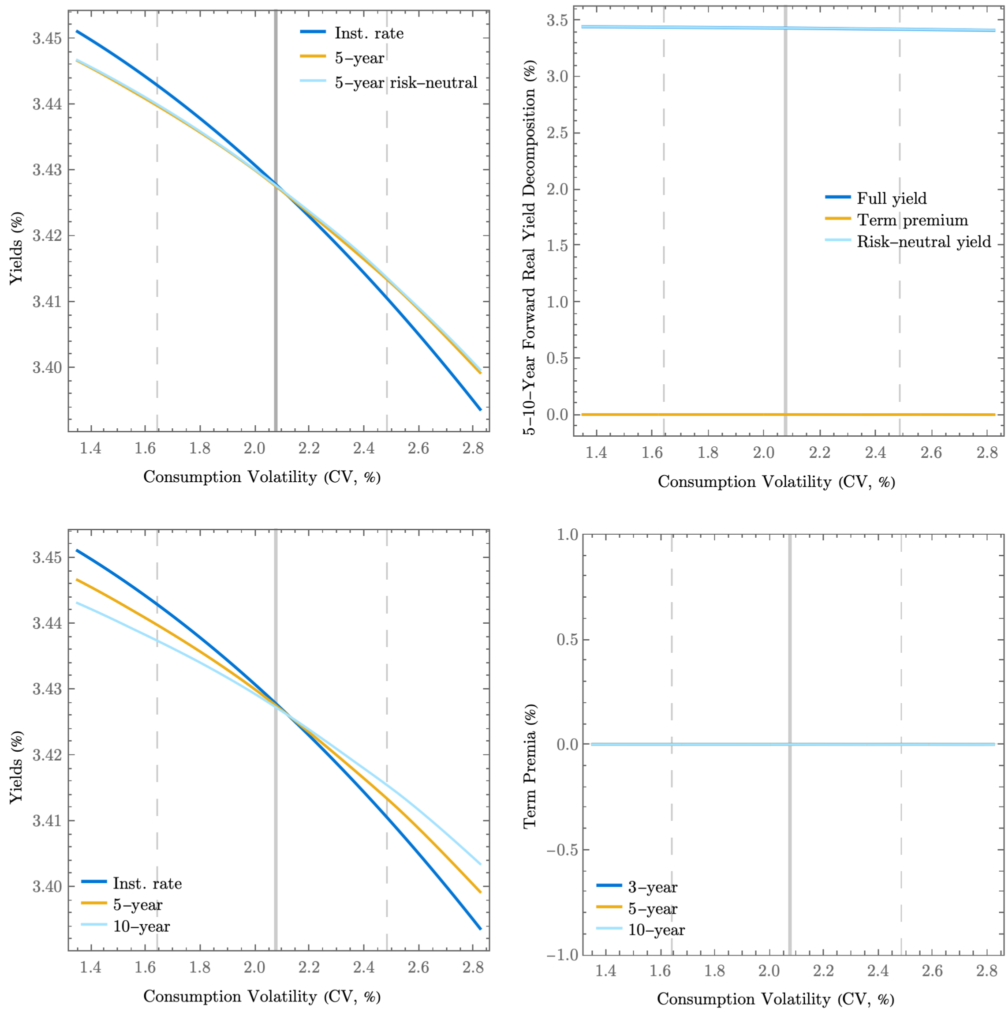

γ=2, ρ=0.012, μ_{ct}=0.0252, σ_{ct}=0.021 $\sqrt{x_t}$, ϕ=0.92, μ_{xt}=μ_x, σ_{xt}=0.13 $\sqrt{x_t}$, ρ_{cx}=−0.5, ψ=1.11, approx. order=8

range$_{\text{low}}$(r$_{2,\text{model}}$)=0.000234865, range$_{\text{high}}$(r$_{2,\text{model}}$)=0.000434075, range(r$_{2,\text{data}}$)=dataRange.

Figure IA.31: Time-varying CV with RU. See Figure IA.1 for plot details.

IA.C.33 RU-CV-HRA, $\gamma = 6$

Term premia have hardly moved.

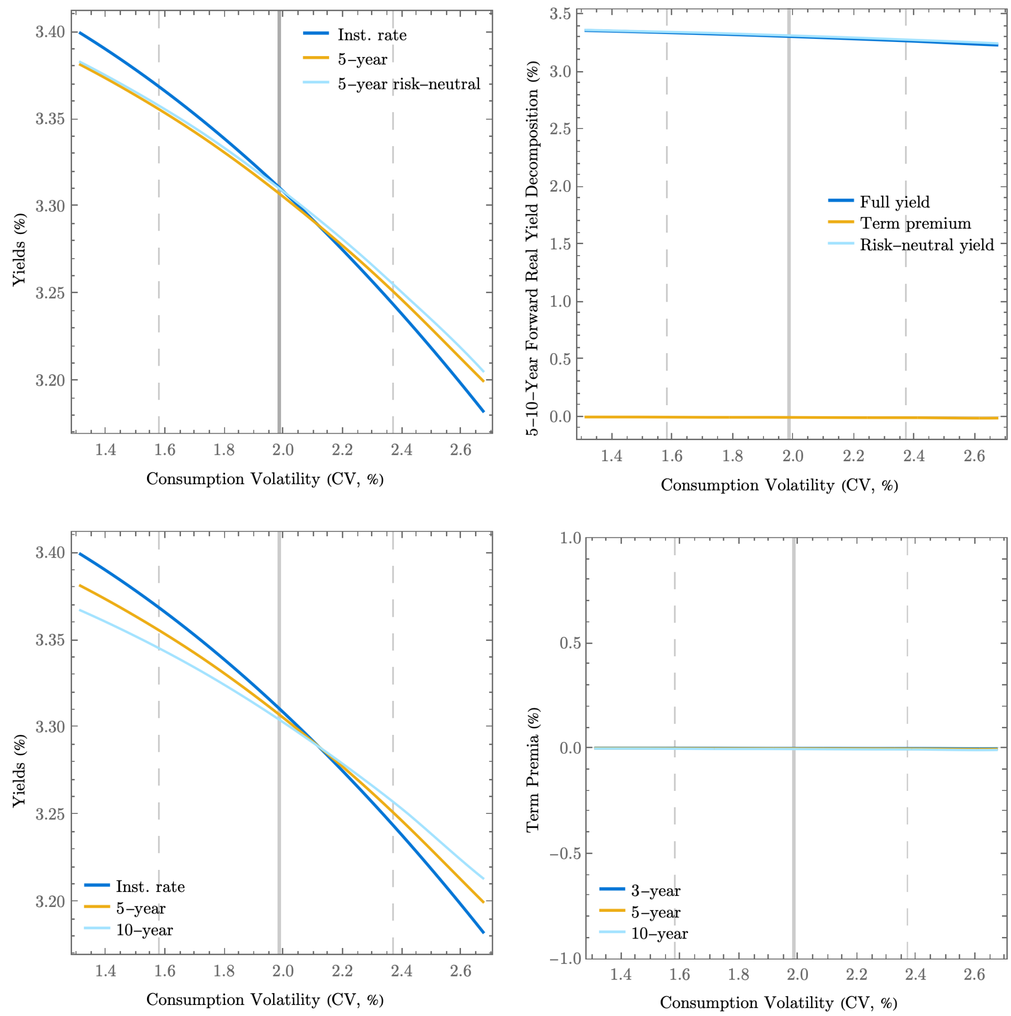

γ=6, ρ=0.012, μ_{ct}=0.0252, σ_{ct}=0.02 $\sqrt{x_t}$, ϕ=0.92, μ_{xt}=μ_x, σ_{xt}=0.13 $\sqrt{x_t}$, ρ_{cx}=−0.5, ψ=1.11, approx. order=8

$\text{range}_{\text{low}}(\text{r}_{2,\text{model}})$=0.000924493, $\text{range}_{\text{high}}(\text{r}_{2,\text{model}})$=0.00168055, $\text{range}(\text{r}_{2,\text{data}})$=0.071748.

Figure IA.32: Time-varying CV with RU and high risk aversion. See Figure IA.1 for plot details.

IA.C.34 RU-CV-HP, $\phi = 0.96$

Term premia have hardly moved; yields become slightly more variable.

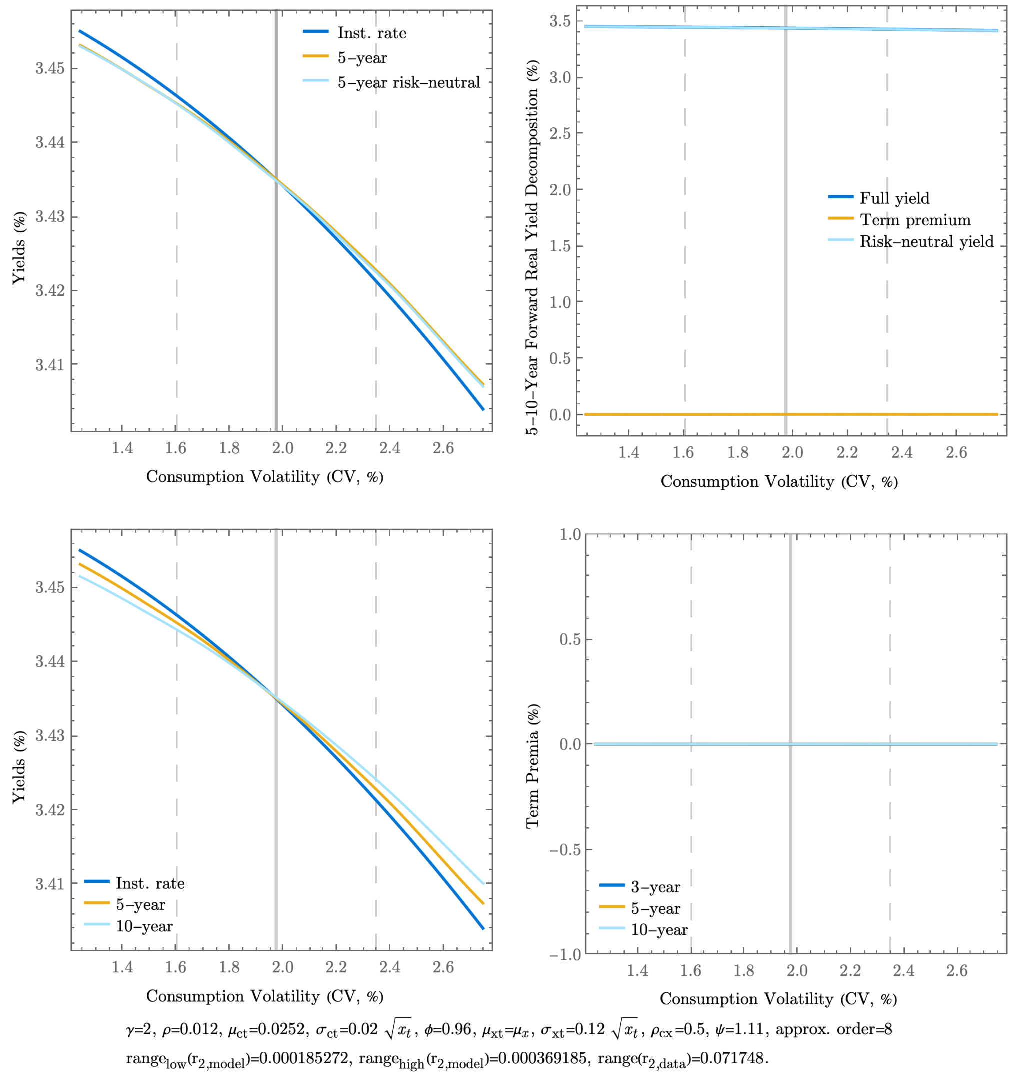

Figure IA.33: Time-varying CV with RU and high persistence. See Figure IA.1 for plot details.

IA.C.35 RU-CV-HIES, $\psi = 1.43$

Term premia have hardly moved; yields become slightly more variable.

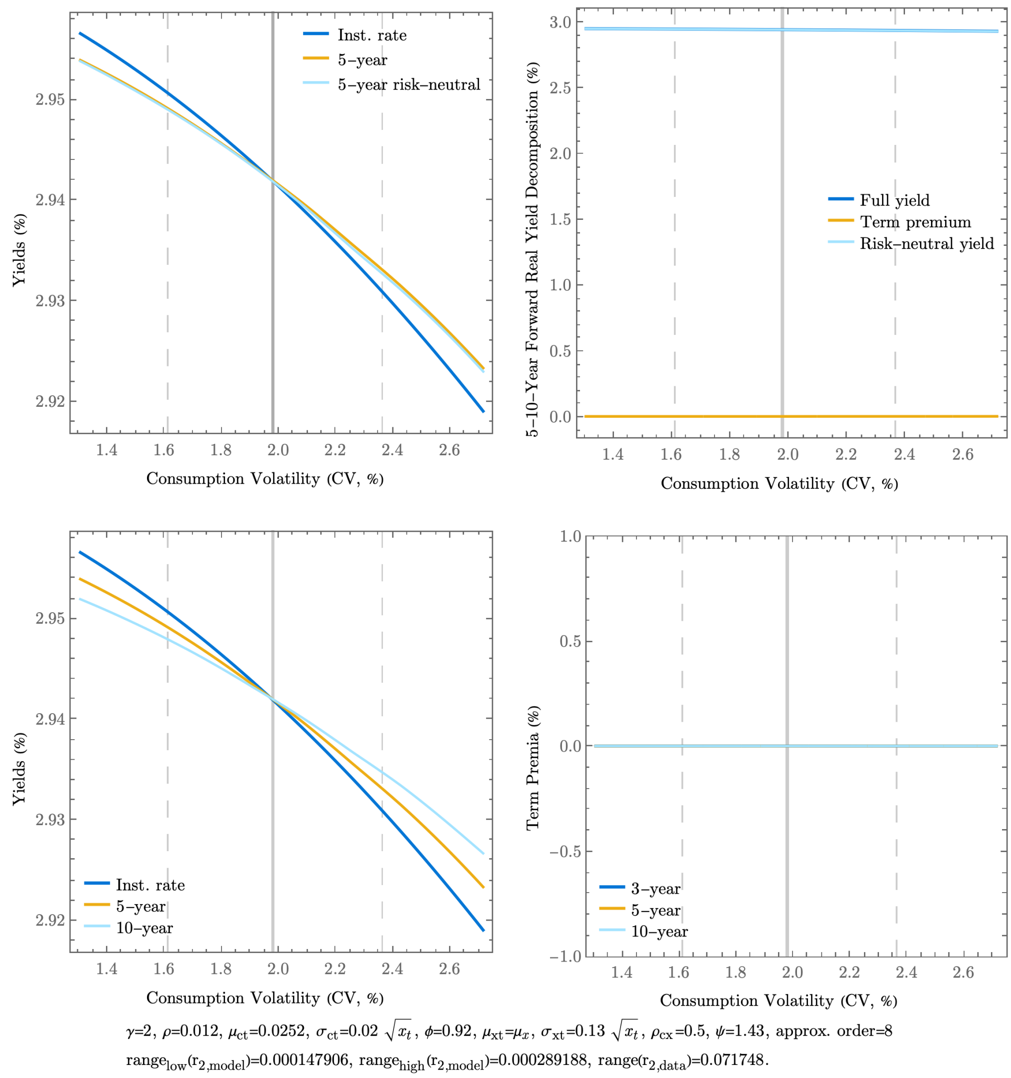

Figure IA.34: Time-varying CV with RU and high IES. See Figure IA.1 for plot details.

IA.C.36 RU-CV-LIES, $\psi = 0.77$

Term premia have hardly moved; yields become slightly more variable.

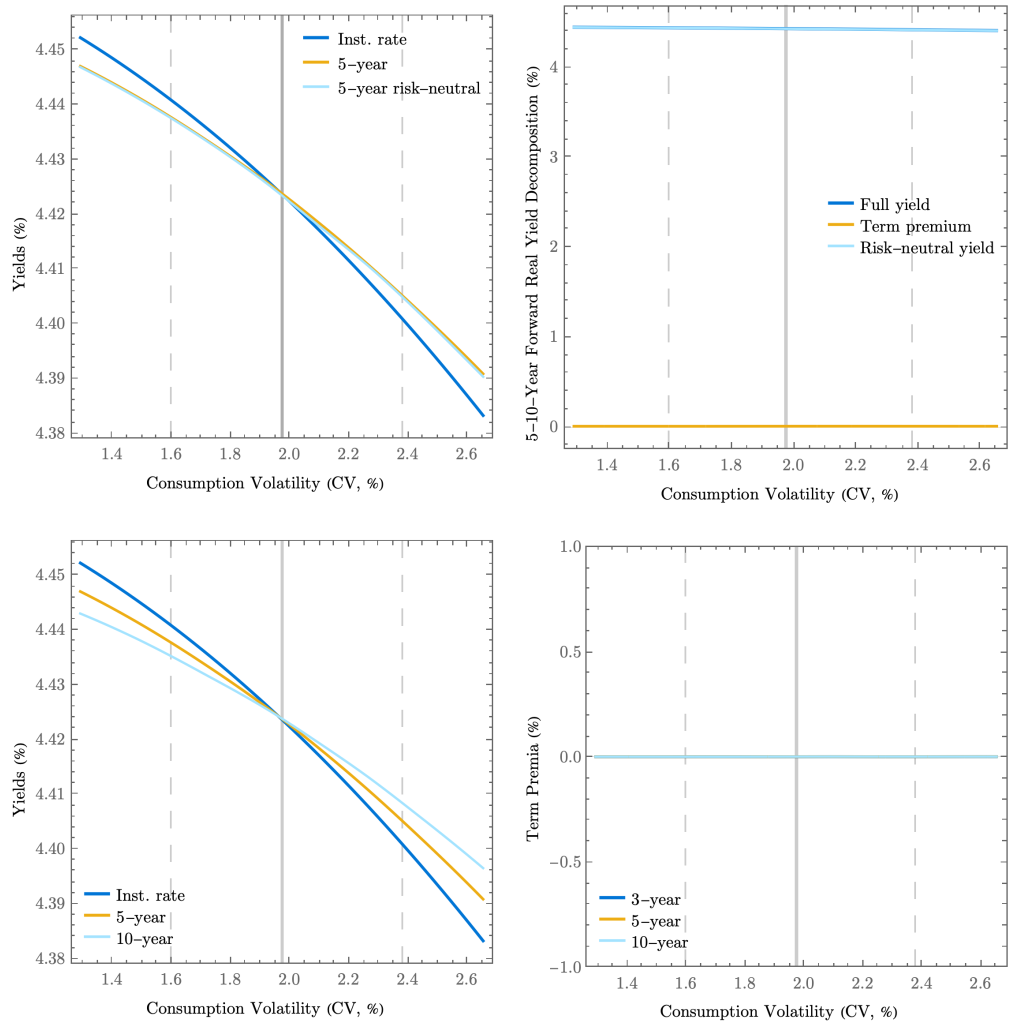

γ=2, ρ=0.012, μ_{ct}=0.0252, σ_{ct}=0.02 $\sqrt{x_t}$, ϕ=0.92, $\mu_{\mathrm{xt}}=\mu_x$, σ_{xt}=0.13 $\sqrt{x_t}$, ρ_{cx}=0.5, ψ=0.77, approx. order=8

$\mathrm{range}_{\mathrm{low}}(\mathrm{r}_{2,\mathrm{model}})$=0.000288099, $\mathrm{range}_{\mathrm{high}}(\mathrm{r}_{2,\mathrm{model}})$=0.000549846, $\mathrm{range}(\mathrm{r}_{2,\mathrm{data}})$=0.071748.

Figure IA.35: Time-varying CV with RU and low IES. See Figure IA.1 for plot details.

IA.C.37 RU-HCV-PCor, $\sigma_{c0} = 0.14$, $\rho_{cx} = 0.5$

Term premia are positive: the first component of A (containing ρ_{cx}) dominates due to the increase in consumption volatility. Nevertheless, term premia are smaller than in the corresponding TSU case because the second component of A remains negative.

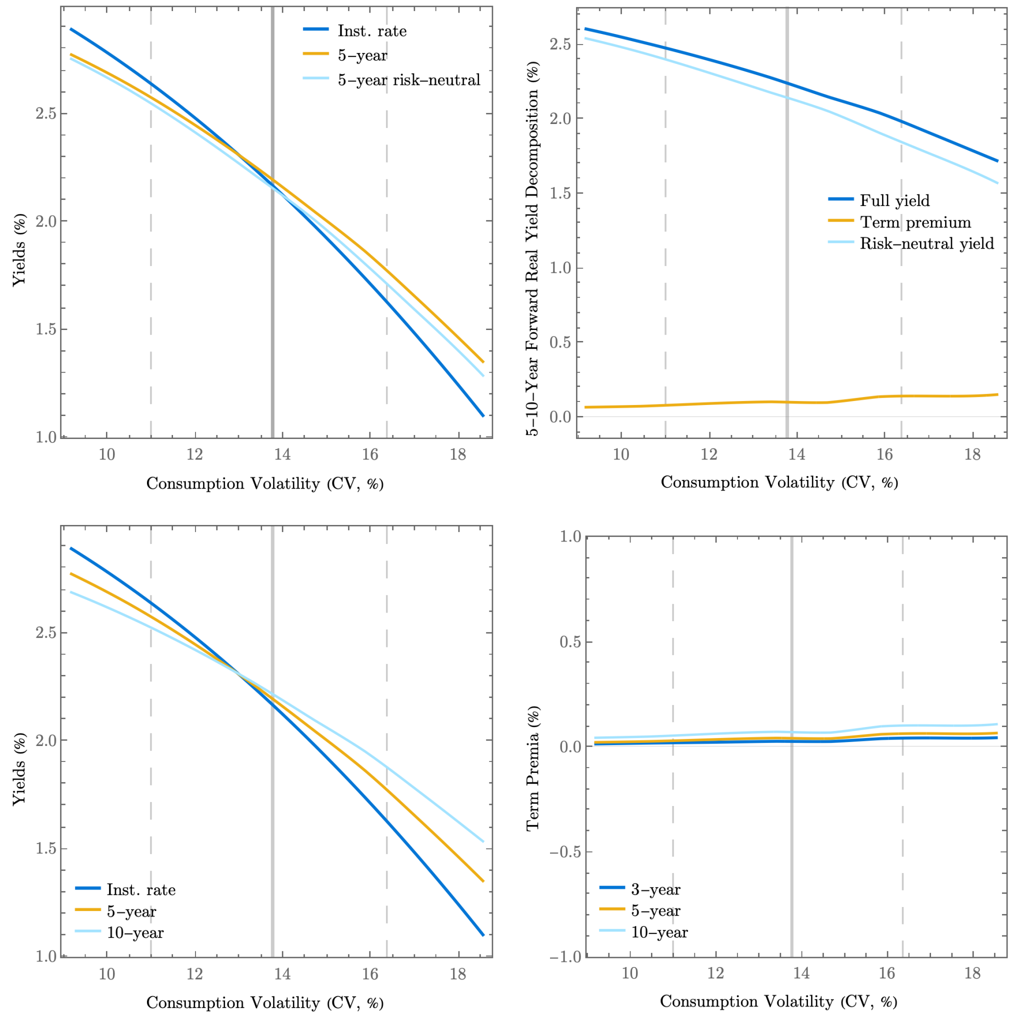

$\gamma=2$, $\rho=0.012$, $\mu_{\mathrm{ct}}=0.0252$, $\sigma_{\mathrm{ct}}=0.14\sqrt{x_t}$, $\phi=0.92$, $\mu_{\mathrm{xt}}=\mu_x$, $\sigma_{\mathrm{xt}}=0.13\sqrt{x_t}$, $\rho_{\mathrm{cx}}=0.5$, $\psi=1.11$, approx. order=8

$\mathrm{range_{low}}(\mathrm{r_{2,model}})=0.0074128$, $\mathrm{range_{high}}(\mathrm{r_{2,model}})=0.0146724$, $\mathrm{range}(\mathrm{r_{2,data}})=0.071748$.

Figure IA.36: Time-varying HCV with RU and positive ρ_{cx}. See Figure IA.1 for plot details.

IA.C.38 RU-HCV-NCor, $\sigma_{c0} = 0.14$, $\rho_{cx} = -0.5$

Both components of A are negative, so term premia are negative and larger in absolute value than in RU-CV.

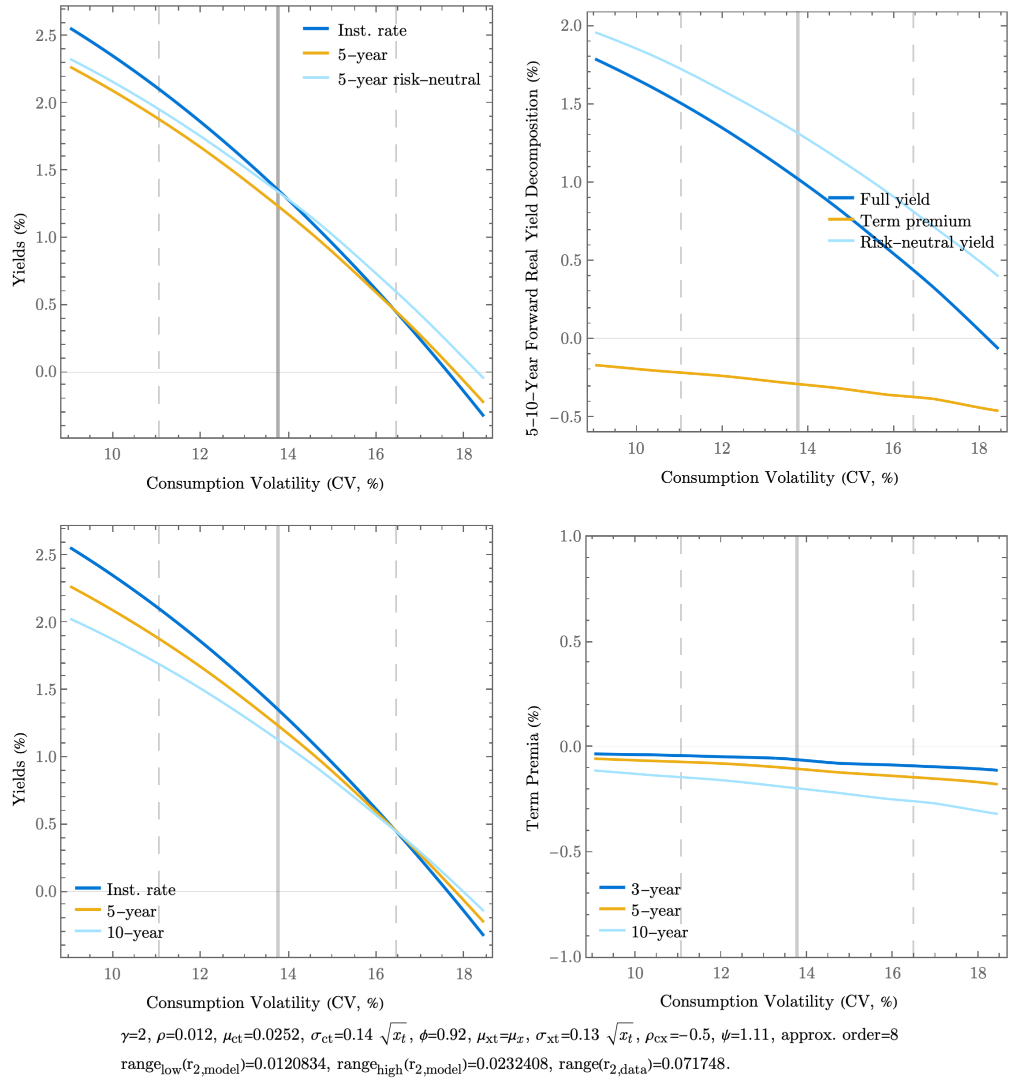

Figure IA.37: Time-varying HCV with RU and negative ρ_{cx}. See Figure IA.1 for plot details.

References

Angeletos, G.-M., Collard, F. and Dellas, H. (2018). Quantifying confidence. *Econometrica*, **86** (5), 1689–1726.

Backus, D. K., Gregory, A. W. and Zin, S. E. (1989). Risk premiums in the term structure: Evidence from artificial economies. *Journal of Monetary Economics*, **24** (3), 371–399.

Bansal, R. and Shaliastovich, I. (2013). A Long-Run Risks Explanation of Predictability Puzzles in Bond and Currency Markets. *The Review of Financial Studies*, **26** (1), 1–33.

— and Yaron, A. (2004). Risks for the long run: A potential resolution of asset pricing puzzles. *The Journal of Finance*, **59** (4), 1481–1509.

Barro, R. J. (2006). Rare disasters and asset markets in the twentieth century. *The Quarterly Journal of Economics*, **121** (3), 823–866.

Bekaert, G., Engstrom, E. and Grenadier, S. R. (2010). Stock and bond returns with moody investors. *Journal of Empirical Finance*, **17** (5), 867–894.

Campbell, J. Y. and Cochrane, J. H. (1999). By force of habit: A consumption-based explanation of aggregate stock market behavior. *Journal of Political Economy*, **107** (2), 205–251.

—, Pflueger, C. and Viceira, L. M. (2020). Macroeconomic drivers of bond and equity risks. *Journal of Political Economy*, **128** (8), 3148–3185.

Collin-Dufresne, P., Johannes, M. and Lochstoer, L. A. (2016). Parameter learning in general equilibrium: The asset pricing implications. *American Economic Review*, **106** (3), 664–698.

Den Haan, W. J. (1995). The term structure of interest rates in real and monetary economies. *Journal of Economic Dynamics and Control*, **19** (5-7), 909–940.

Donaldson, J. B., Johnsen, T. and Mehra, R. (1990). On the term structure of interest rates. *Journal of Economic Dynamics and Control*, **14** (3-4), 571–596.

Duffee, G. R. (2002). Term premia and interest rate forecasts in affine models. *The Journal of Finance*, **57** (1), 405–443.

— (2013). Bond pricing and the macroeconomy. *Handbook of the Economics of Finance*, **2**, 907–967.

Duffie, D. and Epstein, L. G. (1992). Stochastic differential utility. *Econometrica: Journal of the Econometric Society*, pp. 353–394.

Ellison, M. and Tischbirek, A. (2021). Beauty contests and the term structure. *Journal of the European Economic Association*, **19** (4), 2234–2282.

Gabaix, X. (2012). Variable rare disasters: An exactly solved framework for ten puzzles in macro-finance. *The Quarterly Journal of Economics*, **127** (2), 645–700.

Gomez-Cram, R. and Yaron, A. (2021). How important are inflation expectations for the nominal yield curve? *The Review of Financial Studies*, **34** (2), 985–1045.

Hsu, A., Li, E. X. and Palomino, F. (2021). Real and nominal equilibrium yield curves. *Management Science*, **67** (2), 1138–1158.

Jappelli, R., Pelizzon, L. and Subrahmanyam, M. G. (2024). *Monetary Policy, the Yield Curve, and the Repo Market*. Tech. rep., SAFE Working Paper.

Katagiri, M. (2022). Equilibrium yield curve, the phillips curve, and monetary policy. *Journal of Money, Credit and Banking*, **54** (8), 2235–2272.

Kekre, R., Lenel, M. and Mainardi, F. (2024). *Monetary Policy, Segmentation, and the Term Structure*. Tech. rep., National Bureau of Economic Research.

Kliem, M. and Meyer-Gohde, A. (2022). (un) expected monetary policy shocks and term premia. *Journal of Applied Econometrics*, **37** (3), 477–499.

Lettau, M. and Wachter, J. A. (2011). The term structures of equity and interest rates. *Journal of Financial Economics*, **101** (1), 90–113.

Piazzesi, M. and Schneider, M. (2006). Equilibrium yield curves. *NBER Macroeconomics Annual*, **21**, 389–442.

Rietz, T. A. (1988). The equity risk premium a solution. *Journal of Monetary Economics*, **22** (1), 117–131.

Rudebusch, G. D. and Swanson, E. T. (2008). Examining the bond premium puzzle with a DSGE model. *Journal of Monetary Economics*, **55**, S111–S126.

— and — (2012). The bond premium in a DSGE model with long-run real and nominal risks. *American Economic Journal: Macroeconomics*, **4** (1), 105–43.

Schneider, A. (2022). Risk-sharing and the term structure of interest rates. *The Journal of Finance*, **77** (4), 2331–2374.

Tsai, J. (2015). Rare disasters and the term structure of interest rates. *Available at SSRN 2669992*.

— and Wachter, J. A. (2018). Pricing long-lived securities in dynamic endowment economies. *Journal of Economic Theory*, **177**, 848–878.

Vayanos, D. and Vila, J.-L. (2021). A preferred-habitat model of the term structure of interest rates. *Econometrica*, **89** (1), 77–112.

Wachter, J. A. (2006). A consumption-based model of the term structure of interest rates. *Journal of Financial Economics*, **79** (2), 365–399.